THE ASTROPHYSICAL JOURNAL, 307:659–674, 1986 August 15

HYDROSTATIC EVOLUTIONARY SEQUENCES FOR THE NUCLEI OF PLANETARY NEBULAE

P. R. WOOD AND D. J. FAULKNER
Mount Stromlo and Siding Spring Observatories, Australian National University
Received 1985 April 8; accepted 1986 January 4

ABSTRACT

This paper describes a set of evolutionary calculations for nuclei of planetary nebulae. The properties of the nuclei are studied as a function of the following three input parameters: (i) mass of the nucleus, which is set equal to 0.60, 0.70, 0.76, and 0.89 $M_\odot$; (ii) departure phase from the asymptotic giant branch (AGB), which is set at four equally spaced values within the helium shell flash cycle; and (iii) mass loss, which takes a range of forms. We have found evidence for a critical AGB core mass and planetary nebula nucleus mass above which radiation pressure removes all the hydrogen-rich material from the nucleus. We argue that *every* AGB star capable of producing a core mass greater than 0.86 $M_\odot$ will produce a planetary nebula with a helium-rich nucleus (or a supernova if the core mass reaches the Chandrasekhar limiting mass of ~ 1.4 $M_\odot$). Such nuclei will evolve through the planetary nebula phase burning helium before cooling off to become non–DA white dwarfs, unless accretion of hydrogen from the interstellar medium can hide the helium-rich layers. The radiation pressure mechanism may help explain a deficiency in the number of high-luminosity AGB stars apparent in some recent surveys in Magellanic Cloud fields.

For the less massive stars that leave the AGB during the interflash phase, the transition time from the AGB to the planetary nebula region is shown to vary strongly with the phase of the shell flash cycle at which the star leaves the AGB. The transition time can be a large fraction of the post–AGB expansion lifetime of a nebula whose ejection ceased when the star was near a post-flash luminosity minimum.

A detailed comparison of our evolutionary results with observational data is given. There is strong evidence that some recent determinations of the luminosities of planetary nebula nuclei systematically underestimate them by a factor of ~ 3. The masses of planetary nebula nuclei vary from ~ 0.6 $M_\odot$ to greater than ~ 0.8 $M_\odot$. There is little evidence for or against the supposition that planetary nebulae are ejected primarily at a helium shell flash.

Subject headings: nebulae: planetary — stars: evolution — stars: interiors — stars: mass loss

I. INTRODUCTION

The mechanism by which planetary nebula (PN) shells are ejected is still subject to considerable uncertainty. It is generally assumed that the precursors of these objects are low to intermediate mass ($M < 5$ $M_\odot$) asymptotic giant branch (AGB) stars and that the planetary nebula nucleus (PNN) is undergoing a final transition to the white dwarf state. The ejected shell is thought to consist of some or all of the unburnt (although not necessarily uncontaminated), hydrogen-rich material out of which the star was originally formed.

The AGB evolution of low-mass stars is characterized by helium shell flashes (e.g., Schwarzschild and Härm 1965). The periodic onset of helium burning is marked by a thermal runaway, during which the burning rate rises very steeply. Provided the total stellar mass is ~ 3 $M_\odot$ or less, this rapid increase in energy production eventually appears in the stellar envelope as an increased luminosity (see Wood and Zarro 1981, and references therein), so that any given luminosity on the AGB is first achieved as a consequence of one of these He shell flashes.

Planetary nebula formation results from some mass-loss process on the AGB, the details of which are poorly known at present. In general, mass-loss rates on the AGB increase with luminosity and, in some suggested mass-loss processes (e.g., radiation pressure ejection: Faulkner 1970; pulsation mode switch: Jones *et al.* 1983), the mass-loss rate may rise dramatically when the surface luminosity reaches some critical value. Thus one of the first questions to arise concerning PN ejection is whether it occurs at random with respect to phase in this shell flash cycle or predominantly at or about the flash when the surface luminosity rises to a maximum. (In this paper, we define phase in a helium shell flash cycle, ϕ, as the fraction of the time interval between two successive flashes, measured from the instant of maximum helium-burning luminosity in the first of the two.) One of our aims in performing these calculations is to see if the evolution of a PNN is significantly affected by the phase of the shell flash cycle at which ejection occurs.

The most extensively used theoretical calculations of the evolution of PNNi are those of Paczyński (1971). He constructed three AGB–PNN evolutionary sequences, but he obtained his starting models in a somewhat artificial manner. He selected cores of 0.6, 0.8, and 1.2 $M_\odot$ from a flash-suppressed 3 $M_\odot$ AGB sequence and added hydrogen-rich envelopes of 1.2×10^{-3}, 1.4×10^{-4}, and 4×10^{-6} $M_\odot$, respectively. These envelopes are small, so that his starting models were quite far from the AGB at the point of construction (having log $T_{\rm eff}$ between 4.2 and 4.7). Paczyński evolved these starting models to the white dwarf domain without incorporating further mass loss in his calculations. In all three cases the helium shell underwent a flash during the PNN phase but, in view of the artificial nature of the starting models, these results say nothing about whether such a flash will occur during evolution of real PNNi. The main deficiency of the Paczyński tracks, as we see them, is that they do not take into account shell flashing in the precursor stars; this could lead to significant errors in the fading time scale for the model PNNi (where the fading time scale is that for luminosity decrease on the hot part of the evolutionary track).

Härm and Schwarzschild (1975) made the first detailed study of evolution away from the AGB which looked at the effect of an AGB shell flash on PNN evolution. They selected as starting points AGB models of mass 0.65 and 1.00 $M_\odot$ taken at the point of maximum surface luminosity immediately following a single helium shell flash; previous shell flashing had been suppressed in their models. After stripping the envelopes from these models, PNNi of mass ~ 0.63 $M_\odot$ and 0.68 $M_\odot$ were left. It seems to us that these models suffer from the fact that only one shell flash was followed on the AGB in the precursor stars. We have found that in these circumstances the resultant flash is much stronger than normal. The one flash followed by Härm and Schwarzschild in the PNN stage of their tracks exhibited the triple flash form typical of early AGB shell flash cycles (e.g., Gingold 1974).

Schönberner (1979, 1981, 1983) appears to have been the first to make a study of evolution through the AGB and PNN stages in which all the helium shell flashes on the AGB were treated in detail. The models of Schönberner are of low mass ($0.55 < M_{\rm PNN}/M_\odot < 0.64$) and were produced from AGB stars by stellar wind mass loss at the rate prescribed by Reimers (1975). Schönberner appears to have adjusted his calculation so that the PNN sometimes left the AGB at helium flash (1979) and sometimes in the interflash phase (1981), but no systematic study of the effect of ϕ on the subsequent evolution of PNNi was made. However, Iben (1984) has carried out a very detailed study of this particular aspect of the evolution of PNNi, for $0.7 < \phi < 1.0$ in a 0.6 $M_\odot$ model—see also Iben *et al.* (1983). It is in this ϕ range that the nucleus can experience a final shell flash in the PNN domain.

The present paper describes evolutionary calculations for nuclei of planetary nebulae which allow for a greater range of parameters than the calculations of Schönberner or Iben. They have been made using a variety of assumptions regarding (i) the mass of the PNN, (ii) the phase ϕ at which the PNN leaves the AGB, and (iii) the time variation of the mass-loss rate. It is hoped that the comparison of these calculations with sufficiently precise observations, when these are available, will resolve some of the present uncertainties regarding planetary shell ejection. Further discussion of the problems of AGB and PN evolution can be found in Iben and Renzini (1983) and Renzini (1983).

II. CALCULATIONS

For all of our calculations, an artificial mass loss has been incorporated into the Mount Stromlo Stellar Structure Programme (Wood and Zarro 1981, and references therein). We initiated mass loss with the protoplanetary on the AGB and applied it automatically to each model as the evolutionary calculation proceded. Our technique was as follows. After the convergence of each new model, the required mass decrement was derived from the time step used for the model and the prescribed mass-loss rate. This mass decrement was extracted from the surface of the star by appropriate adjustment of the total stellar mass and of the mesh structure. It is well known that the evolution of the core of an AGB star is essentially independent of envelope mass (e.g., Paczyński 1971; Wood and Zarro 1981); thus the structure of the core is not affected by mass loss, and no changes in the mass intervals of the mesh were needed in the interior below $T = 10^7$ K. After adjustment of the envelope mesh, the next model was converged, and so on.

Our first task is to decide what mass-loss rate to adopt at the time the PN mass loss is initiated. In view of the observed mass-loss rates in the likely progenitor objects (type II OH/IR stars: Werner *et al.* 1980; Zuckerman 1980; Jones *et al.* 1983; or extreme carbon stars: Knapp *et al.* 1982), we usually set this at 3×10^{-5} $M_\odot$ yr^{-1}. At this rate, the removal of an envelope of typical PN mass will take ~ 6000 yr. This is comparable with the typical expansion time scales calculated observationally for planetary shells by dividing their radii by their expansion velocities: in general, the shells appear to become ionized after ~ 5000 yr and appear to dissipate to the point of invisibility in the order of 30,000 yr. Some authors (e.g., Härm & Schwarzschild 1975) have argued for using a higher mass-loss rate, to make the adopted ejection time scale substantially shorter than the expansion time scale to the point of shell ionization. It should be remembered, however, that expansion velocities are observed only *after* shell ionization, and that in reality they could be considerably slower in the shell ejection phase, and thus the actual shell formation time scale considerably longer than its apparent value. In particular, the shell ejection may be a discrete dynamical event involving the whole shell mass (rather than a steady state wind); such an event may commence with a slow ejection velocity which is gradually accelerated by some mechanism until, by the time the PNN has become hot enough to ionize the shell, the velocity has acquired the value typically observed in PNe. In fact there is observational evidence that the expansion velocity does increase somewhat with time (Sabbadin and Hamzaoglu 1982; Robinson, Reay, and Atherton 1982). All things considered, an initial mass-loss rate of 3×10^{-5} $M_\odot$ yr^{-1} seems to us to be an appropriate one to adopt.

We define $M_{\rm PNN}$ as the mass of the PNN when all mass loss has effectively ceased; this may, of course, be much less than that which the star's progenitor had on the AGB. Four values of $M_{\rm PNN}$ have been investigated in this study: 0.60, 0.70, 0.76, and 0.89 $M_\odot$. The starting models used were derived from AGB evolutionary sequences (Wood and Zarro 1981) constructed with $M = 2.0$ $M_\odot$ and $(X, Y, Z) = (0.68, 0.30, 0.02)$. Each of the starting models had been through many (>12) shell flashes on the AGB, so they should have been well relaxed thermally to a state similar to that of true planetary nebula precursors. The interior properties (particularly luminosities) of AGB stars are determined almost entirely by the core mass, M_c, rather than the total mass of the star. As usual, we define M_c for an AGB model as the mass interior to the point in the hydrogen-burning shell where the hydrogen abundance has half of its surface value, we define the envelope mass, M_e, as the mass exterior to the same point. The effective temperature is also relatively insensitive to total mass except when M_e falls to a very low value, at which time the star begins to depart from the AGB toward higher temperature. Thus it is feasible to study the evolution of a PNN (with given mass $M_{\rm PNN}$, and which leaves the AGB at given phase ϕ) by extracting a model from an AGB sequence when $M_c = M_{\rm PNN}$ and ϕ has the required value, and then rapidly stripping off just sufficient envelope mass so that (i) the remnant star still resides on the AGB after thermally adjusting its outer structure following this stripping and (ii) the amount of hydrogen left on the remnant is such that, under the influence of the imposed PN mass loss, the envelope will be dissipated in a time short compared with the current interflash period. After some experimentation it was discovered that, for our assumed initial mass-loss rate of $3 \times 10^{-5}\ M_\odot\ \mathrm{yr}^{-1}$, these two criteria were met by stripping the envelope mass to the point at which $M_e X_e = 0.01\ M_{\mathrm{PNN}}$, where X_e is the surface hydrogen abundance.

Another property of AGB models which depends almost entirely on M_c is the interval between successive helium shell flashes. This interflash period decreases quite steeply with increasing M_c, being ~68,500, 29,300, 17,600, and 6000 yr when $M_c = 0.6$, 0.7, 0.76, and 0.89 $M_\odot$, respectively. These intervals should be compared with the shell ejection time scale we are considering (~6000 yr). For the lower end of our range of M_{PNN}, our adopted mass-loss rate is capable of ejecting the entire PN shell over an interval embracing only a fraction of the total ϕ interval of the helium flashing. At the higher end these two time scales are comparable, and the steady wind ejection may continue through *all* ϕ values in the cycle. Nevertheless, evolution on the AGB continues unaffected by mass loss until the envelope mass has been reduced to a very small value ($M_e < 0.01\ M_\odot$) and the star leaves the AGB. For given M_{PNN}, it is the phase ϕ at which the star leaves the AGB that determines subsequent evolution of the PNN, and it is in this sense that ϕ is specified by the above stripping procedure.

We have extracted models from our AGB sequence at those epochs where M_c has reached each of the four values of M_{PNN} selected for study, and for each of these masses four models have been selected with ϕ values of 0.0, 0.25, 0.5, and 0.75. Thus there are 16 different starting models in all, and each of these models has been prepared by very rapidly ($\dot{M} \approx 1.0\ M_\odot\ \mathrm{yr}^{-1}$) stripping it until $M_e X_e = 0.01\ M_{\mathrm{PNN}}$ (as prescribed above). Our PNN evolutionary sequences, using a variety of mass-loss rate variations, have then been commenced from these starting models.

One might envisage two extreme types of mass-loss *duration* associated with PN ejection. At one extreme the cause of the mass loss might be closely associated with the global properties of the AGB star (luminosity, radius, etc.). In this case one might expect that, when the star reaches the AGB tip, mass will be lost from the surface layers of the envelope in a steady state wind and that such mass loss will continue until it results in the global properties of the star becoming sufficiently removed from those of the AGB tip that the mass loss is extinguished. In modeling this possibility one could set the mass-loss rate at the observed value until the PNN has left the AGB and then change it discontinuously to zero.

The second extreme possibility might arise if the cause of the mass loss is associated closely with the composition of the star's remaining outer layers, rather than with the star's global properties. For example, mass loss might continue while any hydrogen-rich material remains on the stellar surface; in this case one might expect the loss of nearly the whole of the hydrogen-rich envelope layers. In modeling this possibility one could set the mass-loss rate at the observed value until the remaining hydrogen in the PNN fell to a negligibly small value.

In § III*a* we report a set of evolutionary sequence calculations for all starting models and for both of these extreme types of PN mass loss. Specifically, the mass-loss types adopted are as follows.

Type A.—Mass-loss rate set at $3 \times 10^{-5}\ M_\odot\ \mathrm{yr}^{-1}$ until the PNN has effectively left the AGB ($\log T_{\mathrm{eff}} = 3.8$), when it is changed to zero.

Type B.—Mass-loss rate set at $3 \times 10^{-5}\ M_\odot\ \mathrm{yr}^{-1}$ and retained at that value until the remaining hydrogen content of the star has been reduced to 10^{-9} by mass fraction. The material at the stellar surface at the completion of the type B mass loss has come from the base of the extinct hydrogen-burning shell (the shell is extinguished by the mass loss). The hydrogen mass fraction in this material is less than 10^{-3}, so that the stellar surface is essentially pure helium. We discontinued the type B mass loss at the 10^{-9} value primarily for computational convenience; the remaining hydrogen has no effect on the star's subsequent evolution. Thus the resulting PNN should evolve as would a helium-rich PNN or a DB white dwarf.

It should be noted that our type A mass loss all occurs while the star remains on or near the AGB, but for type B a fraction of the loss occurs on the AGB and the remainder while the star is evolving into the planetary domain. There is, however, little chance that a PNN would actually be observed while undergoing mass loss at the rate we have assumed, for the following reasons. In both case A and case B the duration of the mass-loss phase (from the prestripped, AGB starting model) is short. If X is the envelope hydrogen mass fraction, the time taken to remove the last ~0.01 $M_\odot$ of hydrogen in our type B is $0.01/(3 \times 10^{-5} X) \approx 490$ yr; for type A the loss phase is even briefer since some hydrogen remains after the mass loss ceases. This brevity means that for neither type would we expect to catch an actual PNN exhibiting the loss. Furthermore, the duration of the loss phase would be insufficient for the dispersal of the ejected material before the ejection is terminated, so that an actual PNN, were it still undergoing either of our prescribed types of mass loss, would be surrounded by a dense, compact, neutral circumstellar shell which would almost certainly obscure the star.

In practice, of course, the actual form of mass loss variation is likely to be intermediate between our two extremes, with the rate commencing at a specific value at the AGB tip and changing (probably decreasing) as the ejection progresses. We have calculated some additional sequences with intermediate mass-loss formulations for our 0.6 $M_\odot$ case.

III. RESULTS

The general form of the results of previous PNN evolutionary calculations is well known. The initial evolution away from the AGB is horizontal in the Hertzsprung-Russell (H-R) diagram; this is followed by a fading phase in which the PNN descends to the white dwarf domain. These features broadly match the corresponding ones on the observational Harman-Seaton (1966; see also Seaton 1966) track for PNNi.

In many instances the PNN traverses this Harman-Seaton (H-S) track in a quiescent way, while burning hydrogen or helium in the appropriate shell source (or both in turn), depending upon the phase of departure from the AGB and the form of mass loss. This burning eventually dies away when the shells approach the stellar surface so closely that they can no longer maintain a high enough temperature to support nuclear reactions. Thereafter it is the gravitational contraction to white dwarf dimensions that provides the star's main energy source. In some instances, however, the model undergoes a final helium shell flash during the PNN evolutionary stage (Schönberger 1979; Iben 1984) because of the PNN leaving the AGB at a ϕ sufficiently close to that of the next He shell flash that the time taken in traversing the PNN domain is shorter than the time to the next flash. If a final flash has not occurred by the time the PNN has ceased its nuclear burning entirely, further shell flashing seems to be permanently inhibited. The

TABLE 1

Properties of the Evolutionary Sequences

TYPE A MASS LOSS

$M_{PNN} = 0.60\ M_\odot$; $\phi = 0.25$

time	$\lg \frac{L}{L_\odot}$	$\lg T_{eff}$	F(H)
-16640*	3.633	3.800	2.8(-3)
-10000	3.701	3.751	2.4(-3)
-3000	3.742	3.807	1.8(-3)
-1000	3.751	3.886	1.6(-3)
0	3.754	4.000	1.5(-3)
1000	3.757	4.149	1.4(-3)
3000	3.761	4.362	1.3(-3)
10000	3.723	4.894	6.4(-4)
30000	2.341	5.063	2.6(-4)
100000	1.816	4.990	2.1(-4)

$M_{PNN} = 0.60\ M_\odot$; $\phi = 0.5$

time	$\lg \frac{L}{L_\odot}$	$\lg T_{eff}$	F(H)
-2717*	3.749	3.800	1.7(-3)
-1000	3.759	3.878	1.6(-3)
-300	3.762	3.929	1.5(-3)
0	3.762	4.000	1.5(-3)
300	3.763	4.059	1.5(-3)
1000	3.766	4.143	1.4(-3)
3000	3.763	4.412	1.2(-3)
10000	3.708	4.940	5.8(-4)
30000	2.359	5.063	2.6(-4)
100000	1.827	4.992	2.1(-4)

$M_{PNN} = 0.60\ M_\odot$; $\phi = 0.75$

time	$\lg \frac{L}{L_\odot}$	$\lg T_{eff}$	F(H)
-1777*	3.786	3.800	1.5(-3)
-1000	3.791	3.842	1.4(-3)
-300	3.792	3.923	1.3(-3)
0	3.792	4.000	1.3(-3)
300	3.792	4.092	1.3(-3)
1000	3.792	4.235	1.2(-3)
3000	3.786	4.523	9.8(-4)
10000	3.578	5.104	3.8(-4)
11760F	2.300	4.932	3.0(-4)

$M_{PNN} = 0.60\ M_\odot$; $\phi = 0$

time	$\lg \frac{L}{L_\odot}$	$\lg T_{eff}$	F(H)
-60*	3.862	3.800	5.8(-4)
0	3.831	4.000	5.8(-4)
30	3.810	4.250	5.8(-4)
300	3.734	4.558	5.8(-4)
1000	3.684	4.696	5.8(-4)
3000	3.540	4.874	5.8(-4)
10000	3.218	5.027	5.7(-4)
14930H	3.219	5.062	5.5(-4)
30000	2.763	5.114	2.9(-4)
100000	1.873	5.003	2.0(-4)

$M_{PNN} = 0.70\ M_\odot$; $\phi = 0.25$

time	$\lg \frac{L}{L_\odot}$	$\lg T_{eff}$	F(H)
-1860*	4.021	3.800	7.3(-4)
-1000	4.042	3.816	6.2(-4)
-300	4.053	3.866	5.2(-4)
0	4.056	4.000	4.7(-4)
300	4.058	4.326	4.2(-4)
1000	4.058	4.715	3.1(-4)
3000	2.788	5.230	7.8(-5)
10000	2.325	5.154	7.2(-5)
30000	1.965	5.091	6.7(-5)
100000	1.551	5.014	6.3(-5)

$M_{PNN} = 0.70\ M_\odot$; $\phi = 0.5$

time	$\lg \frac{L}{L_\odot}$	$\lg T_{eff}$	F(H)
-790*	4.071	3.800	5.2(-4)
-300	4.075	3.844	4.5(-4)
0	4.077	4.000	4.0(-4)
300	4.077	4.418	3.5(-4)
1000	4.064	4.878	2.3(-4)
3000	2.533	5.188	7.3(-5)
10000	2.251	5.141	7.0(-5)
30000	1.940	5.086	6.6(-5)
100000	1.547	5.014	6.3(-5)

$M_{PNN} = 0.70\ M_\odot$; $\phi = 0.75$

time	$\lg \frac{L}{L_\odot}$	$\lg T_{eff}$	F(H)
-743*	4.082	3.800	4.9(-4)
-300	4.086	3.838	4.2(-4)
0	4.086	4.000	3.7(-4)
300	4.085	4.474	3.2(-4)
1000	4.066	4.952	2.0(-4)
3000	2.467	5.178	7.1(-5)
10000	2.234	5.139	6.8(-5)
30000	1.927	5.084	6.5(-5)
100000	1.543	5.011	6.1(-5)

$M_{PNN} = 0.70\ M_\odot$; $\phi = 0$

time	$\lg \frac{L}{L_\odot}$	$\lg T_{eff}$	F(H)
-373*	4.157	3.800	1.9(-4)
0	4.088	4.000	1.9(-4)
30	4.083	4.171	1.9(-4)
300	4.042	4.650	1.9(-4)
1000	3.951	4.946	1.9(-4)
3000	3.715	5.172	1.9(-4)
4333H	3.639	5.227	1.8(-4)
10000	2.745	5.223	8.0(-5)
30000	2.072	5.111	6.8(-5)
100000	1.578	5.019	6.3(-5)

$M_{PNN} = 0.76\ M_\odot$; $\phi = 0.25$

time	$\lg \frac{L}{L_\odot}$	$\lg T_{eff}$	F(H)
-675*	4.178	3.800	3.4(-4)
-300	4.182	3.832	2.7(-4)
0	4.184	4.000	2.1(-4)
300	4.180	4.762	1.5(-4)
1000	3.578	5.415	3.9(-5)
3000	2.434	5.213	3.8(-5)
10000	2.129	5.156	3.6(-5)
30000	1.819	5.096	3.6(-5)
100000	1.442	5.022	3.5(-5)

$M_{PNN} = 0.76\ M_\odot$; $\phi = 0.5$

time	$\lg \frac{L}{L_\odot}$	$\lg T_{eff}$	F(H)
-621*	4.194	3.800	3.1(-4)
-300	4.197	3.828	2.5(-4)
0	4.198	4.000	1.9(-4)
300	4.189	4.867	1.2(-4)
1000	2.514	5.232	3.5(-5)
3000	2.253	5.180	3.5(-5)
10000	2.048	5.140	3.4(-5)
30000	1.787	5.089	3.4(-5)
100000	1.431	5.016	3.3(-5)

$M_{PNN} = 0.76\ M_\odot$; $\phi = 0.75$

time	$\lg \frac{L}{L_\odot}$	$\lg T_{eff}$	F(H)
-594*	4.200	3.800	3.0(-4)
-300	4.201	3.827	2.4(-4)
0	4.202	4.000	1.8(-4)
300	4.192	4.898	1.2(-4)
1000	2.442	5.219	3.4(-5)
3000	2.217	5.173	3.4(-5)
10000	2.028	5.136	3.4(-5)
30000	1.781	5.084	3.3(-5)
100000	1.436	5.020	3.2(-5)

$M_{PNN} = 0.76\ M_\odot$; $\phi = 0$

time	$\lg \frac{L}{L_\odot}$	$\lg T_{eff}$	F(H)
-493*	4.266	3.800	1.6(-4)
0	4.168	4.000	1.6(-4)
30	4.162	4.237	1.6(-4)
300	4.112	4.817	1.6(-4)
1000	3.967	5.151	1.6(-4)
1655H	3.957	5.217	1.5(-4)
3000	3.503	5.372	5.2(-5)
10000	2.367	5.202	3.8(-5)
30000	1.905	5.113	3.6(-5)
100000	1.474	5.029	3.5(-5)

$M_{PNN} = 0.89\ M_\odot$; $\phi = 0.25$

time	$\lg \frac{L}{L_\odot}$	$\lg T_{eff}$	F(H)
-550*	4.362	3.800	1.9(-4)
-100	4.365	3.858	8.5(-5)
0	4.365	4.000	6.1(-5)
300	2.774	5.357	1.1(-5)
1000	2.551	5.311	1.1(-5)
3000	2.342	5.269	1.1(-5)
10000	2.051	5.209	1.0(-5)
30000	1.752	5.145	1.0(-5)
100000	1.323	5.053	1.0(-5)

$M_{PNN} = 0.89\ M_\odot$; $\phi = 0.5$

time	$\lg \frac{L}{L_\odot}$	$\lg T_{eff}$	F(H)
-541*	4.367	3.800	1.9(-4)
-100	4.368	3.858	8.3(-5)
0	4.368	4.000	5.8(-5)
300	2.655	5.334	1.0(-5)
1000	2.550	5.311	1.0(-5)
3000	2.281	5.256	1.0(-5)
10000	2.032	5.204	1.0(-5)
30000	1.743	5.143	1.0(-5)
100000	1.318	5.052	1.0(-5)

$M_{PNN} = 0.89\ M_\odot$; $\phi = 0.75$

time	$\lg \frac{L}{L_\odot}$	$\lg T_{eff}$	F(H)
-537*	4.367	3.800	1.9(-4)
-100	4.369	3.858	8.2(-5)
0	4.369	4.000	5.7(-5)
300	2.642	5.332	1.1(-5)
1000	2.490	5.300	1.0(-5)
3000	2.296	5.260	1.0(-5)
10000	2.024	5.203	1.0(-5)
30000	1.741	5.143	1.0(-5)
100000	1.318	5.052	1.0(-5)

TYPE B MASS LOSS

$M_{PNN} = 0.60\ M_\odot$; $\phi = 0.5$

time	$\lg \frac{L}{L_\odot}$	$\lg T_{eff}$	F(H)
-5	3.750	3.800	1.7(-3)
0	3.740	4.000	1.6(-3)
10	3.724	4.501	1.2(-3)
51*	2.159	5.048	1.0(-9)
300	2.567	5.155	-
1000	2.487	5.139	-
3000	2.432	5.130	-
10000	2.308	5.112	-
30000	2.045	5.069	-
100000	1.644	4.999	-

$M_{PNN} = 0.60\ M_\odot$; $\phi = 0$

time	$\lg \frac{L}{L_\odot}$	$\lg T_{eff}$	F(H)
-4	3.862	3.800	5.8(-4)
0	3.852	4.000	4.6(-4)
10	3.838	4.842	1.2(-4)
17*	3.806	5.124	1.0(-9)
300	3.729	5.142	-
1000	3.684	5.167	-
3000	3.534	5.198	-
10000	3.169	5.214	-
30000	2.409	5.134	-
100000	1.715	5.015	-

$M_{PNN} = 0.70\ M_\odot$; $\phi = 0.5$

time	$\lg \frac{L}{L_\odot}$	$\lg T_{eff}$	F(H)
-4	4.071	3.800	5.3(-4)
0	4.067	4.000	4.2(-4)
10	3.982	5.200	1.3(-4)
16*	2.799	5.274	1.0(-9)
300	2.645	5.251	-
1000	2.560	5.235	-
3000	2.427	5.210	-
10000	2.187	5.165	-
30000	1.893	5.107	-
100000	1.518	5.033	-

$M_{PNN} = 0.70\ M_\odot$; $\phi = 0$

time	$\lg \frac{L}{L_\odot}$	$\lg T_{eff}$	F(H)
-4	4.157	3.800	1.9(-4)
0	4.152	4.000	7.4(-5)
3	4.154	5.130	4.5(-6)
5*	3.136	5.191	1.0(-9)
300	4.100	5.252	-
1000	3.998	5.310	-
3000	3.745	5.370	-
10000	2.625	5.248	-
30000	2.020	5.132	-
100000	1.549	5.038	-

$M_{PNN} = 0.76\ M_\odot$; $\phi = 0.5$

time	$\lg \frac{L}{L_\odot}$	$\lg T_{eff}$	F(H)
-4	4.194	3.800	3.1(-4)
0	4.190	4.000	1.9(-4)
3	4.187	4.961	1.1(-4)
8*	2.912	5.346	1.0(-9)
300	2.452	5.250	-
1000	2.338	5.226	-
3000	2.221	5.202	-
10000	2.026	5.161	-
30000	1.781	5.110	-
100000	1.428	5.038	-

$M_{PNN} = 0.76\ M_\odot$; $\phi = 0$

time	$\lg \frac{L}{L_\odot}$	$\lg T_{eff}$	F(H)
-5	4.266	3.800	1.6(-4)
0	4.261	4.000	3.2(-5)
1	4.269	5.093	6.8(-6)
2*	4.247	5.277	1.0(-9)
300	4.201	5.343	-
1000	4.064	5.418	-
3000	3.322	5.406	-
10000	2.293	5.218	-
30000	1.888	5.135	-
100000	1.467	5.047	-

$M_{PNN} = 0.89\ M_\odot$; $\phi = 0.5$

time	$\lg \frac{L}{L_\odot}$	$\lg T_{eff}$	F(H)
-6	4.367	3.800	1.9(-4)
0	4.364	4.000	5.9(-5)
1	4.360	5.037	3.6(-5)
3*	3.263	5.492	1.0(-9)
300	2.561	5.335	-
1000	2.410	5.302	-
3000	2.277	5.274	-
10000	2.026	5.219	-
30000	1.740	5.157	-
100000	1.318	5.063	-

$M_{PNN} = 0.89\ M_\odot$; $\phi = 0$

This model was stripped of all hydrogen before the sequence was commenced; see text.

time	$\lg \frac{L}{L_\odot}$	$\lg T_{eff}$	F(H)
0	4.729	4.000	zero
300	4.397	5.540	-
1000	3.284	5.485	-
3000	2.532	5.331	-
10000	2.091	5.235	-
30000	1.759	5.163	-
100000	1.322	5.066	-

precise circumstances under which a final helium flash occurs have been carefully explored in a 0.6 $M_\odot$ model by Iben (1984).

The main object of this study is to explore the properties of the evolution of PNNi as a function of the several variables mentioned above. A few of our evolutionary tracks encountered in a final flash, and these will be described in § III*c*.

a) *The Evolutionary Sequences*

The application of our type A and B forms of mass loss to all of our starting models resulted in a set of 32 evolutionary sequences. Some properties of selected sequences are given in Table 1. We found that, with one exception, the evolutionary tracks resulting from the starting models at $\phi = 0.25$ and 0.75 were generally similar to those resulting from the models at $\phi = 0.50$; thus, it is necessary to discuss in detail only the $\phi = 0.50$ sequences and those starting at rising light in the flash (near $\phi = 0$); we will refer to these as the (helium) interflash and flash sequences, respectively. The exception referred to above occurred in the case A mass-loss evolution from the 0.6 $M_\odot$, $\phi = 0.75$ starting model; this sequence encountered a final mixing helium shell flash (see § III*c*). There are also some time scale differences between the $\phi = 0.25$, 0.5, and 0.75 tracks which will be discussed in § III*d*.

It was found to be impossible, for either type A or B mass loss, to produce complete converged sequences commencing with the 0.89 $M_\odot$, helium flash starting model; the reasons for this are described in the next subsection. Thus there are 14 sequences which we will discuss and compare in some detail. The Hertzsprung-Russell diagrams for these are shown in Figure 1. In all cases the tracks show the well-known horizontal and fading segments of the H-S sequence.

A convenient way of displaying the evolutionary time scales of the PNN sequences is in the (M_V, time) plane. This is because the bolometric correction causes lines of constant M_V to be reasonably orthogonal to the H-S track in the H-R diagram. Abell (1966) first explored the location of actual PNNi in an equivalent of the (M_V, t) plane, and such plots may be used to compare observed and theoretical timescales (see § IV). In making these comparisons it is usual to set the theoretical zero point of time at some arbitrarily chosen log $T_{\rm eff}$ value on the evolutionary tracks; in our case the times indicated in Figure 1 have their zero at log $T_{\rm eff} = 4.0$. This means that all comparisons in the (M_V, t) plane must be based on the *slopes* of the loci and not on the *absolute values* of the time themselves. Our lack of knowledge concerning the actual mechanism and duration of the shell ejection makes all such comparisons between theory and observation uncertain to within a constant time displacement (which may well vary with $M_{\rm PNN}$). The (M_V, time) results in our tracks are shown in Figure 2. In view of the zero point uncertainty we have arbitrarily arranged the loci to coincide at $M_V = 0$ (as closely as clarity permits). Panels *a–d* of Figure 2 give the evolutionary time scales of the tracks shown in the corresponding panels of Figure 1.

The following features may be noted by comparing the tracks of Figures 1 and 2.

1. The higher the mass of the PNN, the hotter, the more luminous, and the more rapid is its evolution. In particular, in almost all cases there is a marked increase in the time required for the PNN to fade from $M_V = 0$ to $M_V = 6$ as we go to lower $M_{\rm PNN}$; the only exception is the case described in the next paragraph.

2. For the tracks leaving the AGB at the interflash phase, and with strong mass loss continuing into the PNN region (type B), the evolution along the horizontal portion of the H-S track is so rapid that virtually all of the life of the PNN is spent at low luminosities ($M_V > 6$), irrespective of $M_{\rm PNN}$.

3. Terminating the mass loss at log $T_{\rm eff} = 3.8$ (type A) for the interflash sequences has little effect on the 0.76 and 0.89 $M_\odot$ tracks, but markedly increases the time spent on the horizontal part of the H-S track as we go to smaller masses.

4. Causing the PNN to leave the AGB at a He shell flash increases the time spent at higher luminosities, particularly for the higher masses.

5. The time scales of the helium flash sequences have less sensitivity to the presence or absence of continued mass loss into the PNN region (type A or B) than do those departing in the interflash phase, although the sense of the effect (longer evolutionary time scales for type A mass loss) is still the same.

6. In general, the luminosities of PNN fade relatively rapidly initially, but the rate of luminosity decline decreases markedly when log $L/L_\odot$ drops to ~ 2.6. Schönberner (1981) and Iben and Tutukov (1984) also noted this type of behavior in their models.

7. For intermediate ages since ejection (~ 3000 yr), the time taken for the luminosity to decline to a given value in the interflash sequences does not seem to decrease with increasing mass beyond ~ 0.8 $M_\odot$; e.g., both the 0.76 and 0.89 $M_\odot$ tracks decay to $L \approx 180$ $L_\odot$ after 3000 yr. If continued to even higher masses, this result means that all PNNi with $M > 0.8$ $M_\odot$ will have similar detection probabilities. The earlier results of Paczyński (1971) suggest a smooth decrease in detection probability (which we equate to lifetime as a PN with $L > 100$ $L_\odot$) with increasing mass. Calculations for higher mass ranges than considered herein are desirable to check time scales beyond the upper mass limit of our calculations (0.89 $M_\odot$). Such calculations would, however, have to be performed using different techniques to those of this study (see § III*b* below).

For the helium flash sequences calculated with type A mass loss, the helium-burning evolution eventually gives way to hydrogen-burning again in the high effective temperature region (see Fig. 1*b*). When this occurs there is a temporary increase in luminosity. Such behavior has been noticed previously (e.g., Härm and Schwarzschild 1975; Iben 1984). Hydrogen reignition does not occur for the helium flash sequences calculated with type B mass loss (Fig. 1*d*) because the continuation of mass loss into the PNN domain has left insufficient hydrogen in the envelope. For the 0.6 $M_\odot$ case, for instance, the star in Figure 1*b* has 5.5×10^{-4} of its mass remaining as hydrogen when hydrogen burning takes over, whereas the hydrogen fraction in the 0.6 $M_\odot$ star in Figure 1*d* has already been depleted to 10^{-9} by the end of its horizontal evolution.

For all the sequences calculated with type A mass loss the PNN still retains typically 10^{-5}–10^{-4} of its mass as hydrogen when nuclear burning via the CN cycle finally ceases on the descent to the white dwarf domain. The change from the continuous to the dotted section of track in Figure 1*a*–1*b* indicates

Notes to Table 1

F(*H*) is the fraction of the star (by mass) remaining as hydrogen. An asterisk (*) denotes the epoch at which the mass-loss rate changed from $3 \times 10^{-5} M_\odot$ yr^{-1} to zero. H denotes the epoch at which hydrogen burning first exceeds helium burning again for PNNi which leave the AGB at helium flash. *F* denotes that a final mixing helium shell flash occurred at this epoch.

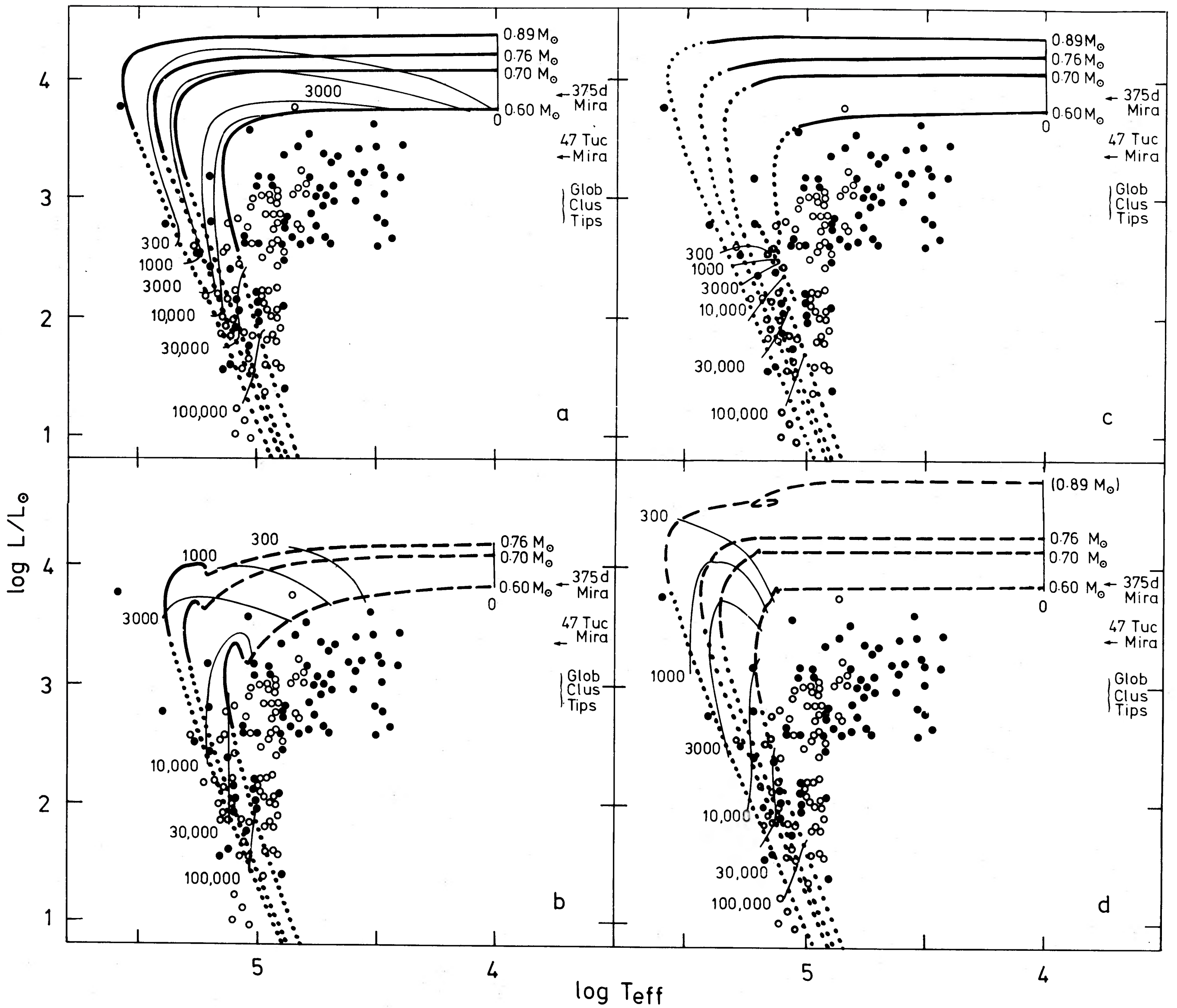

FIG. 1.—Evolutionary tracks for nuclei of planetary nebulae with various masses (as shown). The PN shell ejection on the AGB has been assumed to occur: (1) midway between helium shell flashes (*top panels*), or (2) at rising surface luminosity during a flash (*bottom panels*). In all cases the nuclei were subjected to mass loss at the rate of 3×10^{-5} $M_{\odot}$ yr^{-1} while in the vicinity of the AGB (until log $T_{eff} = 3.8$); thereafter the mass-loss rate was set to zero (type A, *left panels*) or continued at 3×10^{-5} $M_{\odot}$ yr^{-1} until the fraction of the star's mass remaining as hydrogen fell to 10^{-9} (type B, *right panels*); in panels *c* and *d* the point at which mass loss ceased lies very close to the 300 yr locus on each track. Top track in panel *d* has been evolved from the 0.89 $M_{\odot}$ shell flash starting model after all surface hydrogen had been removed. Hydrogen-burning phases are shown as thick lines, helium-burning phases as broken lines, and gravitational contraction phases as dotted lines. Thin lines connect points of equal evolutionary time (marked in years) from the log $T_{eff} = 4.0$ point. The observational Harman-Seaton sequence is defined by the data of Pottasch (1983; *filled circles*) and of Kaler (1983; *open circles*). Luminosities of globular cluster red giant tips, of the 47 Tuc Miras, and of typical Galactic disk Miras are also shown.

the point where the energy production due to the CN cycle falls below that due to gravitational contraction; nuclear burning has become virtually extinct at the lowest luminosities shown in the figure, although hydrogen burning via the *p-p* chain may occur at still lower luminosities; see Iben and Tutukov (1984).

As we have noted, our mass-loss types A and B are likely to be limiting cases between which lies the actual form of mass loss in planetary shell ejection. Accordingly, the two sets of sequences described above are also likely to be limiting cases. We have calculated a series of test sequences with intermediate mass-loss rates and have found, as expected, that the evolutionary time scales for these models lie between those for sequences with mass loss of types A and B.

b) *Upper Mass Limits for Hydrogen-rich PNNi*

As remarked above, the sequences starting with 0.89 $M_{\odot}$ models at helium flash eventually failed to converge; this occurred when the mass loss had just started to make the star evolve off the AGB. It was caused by the radiation pressure becoming so large in the envelope that it supplied all the pressure support required by the model; thus the gas pressure was forced to zero. The problem region was at the base of the convective envelope, at the innermost points having the full hydrogen-rich surface composition. In this region convection carries only a very small fraction of the energy flux (and the region adjoining the base of the convective envelope is, of course, fully radiative). Thus we need consider energy transport by radiation alone. The cause of the structure problems in these models can be explained as follows. From the equation of hydrostatic equilibrium,

$$\frac{dP}{dr} = -\frac{GM_r}{r^2}\rho,$$

and the radiative transfer equation in the form

$$\frac{dP_{\rm rad}}{dr} = -\frac{\kappa\rho L_r}{4\pi c r^2},$$

we find

$$\frac{dP_{\rm rad}}{dP} = \frac{\kappa L_r}{4\pi c G M_r}. \quad (1)$$

For the region between the core and the part of the envelope where convection becomes efficient in a star on the AGB (or for the *entire* envelope of a PNN which has left the AGB), we find that $M_r \approx M_c$ and $L_r \approx L$, where M_c is the core mass. If equation (1) is integrated inward over a few pressure scale heights through the region of the star where convection carries little or no energy flux we find

$$\frac{P_{\rm rad}}{P} = 1 - \beta \approx \frac{\langle\kappa\rangle L}{4\pi c G M_c}, \quad (2)$$

where $\langle\kappa\rangle = P^{-1}\int_0^P \kappa dP$, and β is the ratio of gas to total pressure. (The reason for the approximate rather than exact equality in eq. [2] is that there is an additional term involving a constant of integration; this extra term becomes insignificant after integration through a few pressure scale heights.) Since, for the region we are considering in the star, κ is approximately constant (at the electron scattering opacity for the envelope composition), equation (2) holds very well locally with $\langle\kappa\rangle$ replaced by the local κ value. The domain of validity of equation (2) includes the base of the convective envelope itself since

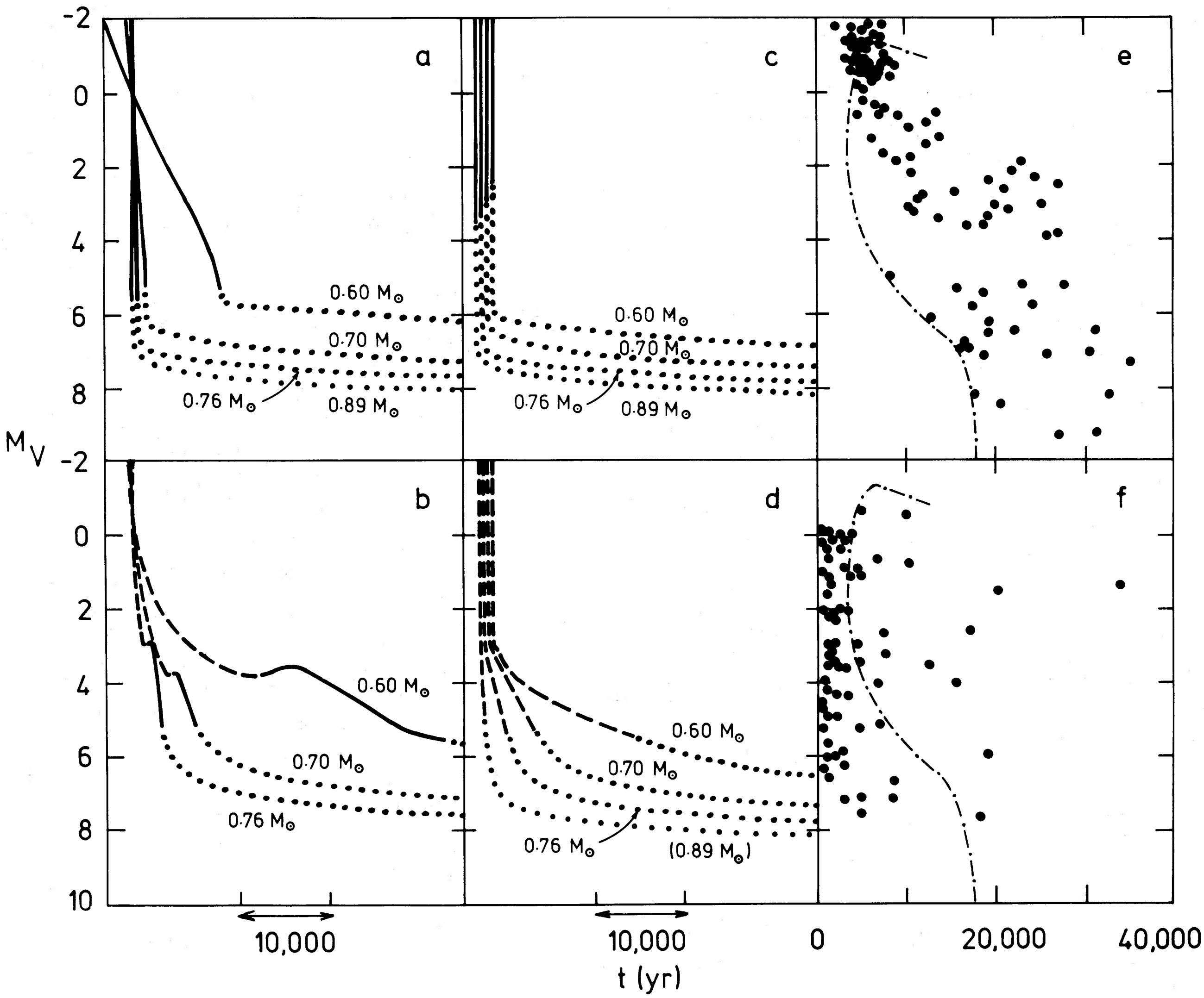

FIG. 2.—(M_V, time) diagrams for the PNN evolutionary tracks and for observational results based on shell expansion time scales. Panels *a–d* show the results for the same sequences as in the corresponding panels of Fig. 1. Hydrogen-burning phases are shown as thick lines, helium-burning phases as broken lines, and gravitational contraction phases as dotted lines. Panels *e* and *f* give the observational results for PNNi obtained by Schönberner (1981) and by Pottasch (1983), respectively; the dot-dash curves indicate Schönberner's boundary, above and to the left of which the PNe are optically thick with respect to Lyman photons.

there are quite a few pressure scale heights of formally convective region above the base of the convective envelope where convection carries only a small fraction (less than a few percent) of the total energy flux. In fact, β has its minimum value at the base of the convective envelope; in luminous AGB stars $\beta \ll 1$ there.

Now suppose a luminosity pulse from a helium shell flash increases L in equation (2) beyond the local Eddington limit, $L_{\rm Ed} = 4\pi cGM_c/\langle\kappa\rangle$: what will happen? To investigate this problem, we have made a series of detailed envelope integrations in stars of core mass 0.89 $M_\odot$, various total masses (to cover the development from the AGB to the PNN stage), and with luminosities up to $L_{\rm Ed}$. Such integrations can be made without any knowledge of the structure of the core; all that is required is knowledge of the core mass (e.g., Keeley 1970*a*). The method of calculation is as follows: a luminosity, total mass, and $T_{\rm eff}$ value are chosen, and the equations of hydrostatic equilibrium are integrated inward beyond the base of the convection region, where the pressure rises rapidly. The mass interior to this region is the core mass, which must be equal to the M_c value for the AGB star which is being modeled; $T_{\rm eff}$ is adjusted until the correct M_c value is obtained. The analytic fit to opacity given by Iben (1975) was used in these calculations rather than the tabular values used in the stellar evolution program to ensure smoothness in critical limiting cases.

Some results of these envelope integrations are shown in Figure 3 for stars of 2.0 $M_\odot$ and 0.9 $M_\odot$. The 2.0 $M_\odot$ star is meant to represent a typical PN precursor star while still on the AGB, while the 0.9 $M_\odot$ star is close to leaving the AGB because of its small envelope mass. The luminosity range was chosen to approximate the range in surface luminosity experienced by an AGB star with $M_c = 0.89$ $M_\odot$ during a helium shell flash cycle. For both the 0.9 and 2 $M_\odot$ stars, the minimum value of β in the envelope matches the estimate given by equation (2) very well. The difference in β values for the two stellar masses is due to the fact that κ is generally larger at and below the base of the convective envelope in the lower mass model. As $L \to L_{\rm Ed}$, the convection moves deeper into the star until in the near-limiting case the convection reaches below the region which would be occupied by the helium-burning shell in the core ($r \approx 0.01$ $R_\odot$). At this point, the assumption that the core and envelope can be treated separately has clearly broken down. We suggest that, in a real star, a hydrodynamic expansion of the envelope of the star occurs at this point; and that the convergence failure in our hydrostatic evolutionary calculations results from the lack of existence of a hydrostatic solution. It is likely that dredge-up of processed material from core to envelope will occur copiously in AGB stars approaching this phase.

The results shown in Figure 3 are qualitatively similar for the 0.9 $M_\odot$ and 2.0 $M_\odot$ models. However, as mentioned above, the minimum value of β is generally smaller in the 0.9 $M_\odot$ models because of the higher opacity at the base of the convective envelope in the low-mass models. The decrease in density and increase in opacity at the base of the convective envelope as envelope mass decreases has the important effect that, if an AGB star has reached the stage where $L \approx L_{\rm Ed}$ at the base of its envelope, removal of mass from the star will cause $L_{\rm Ed}$ at the base of the envelope to decrease, and a situation may thus arise where the existing luminosity exceeds the new Eddington limit, resulting in complete envelope ejection. It appears that this is the situation which has arisen in the case of our 0.89 $M_\odot$ model. The 2 $M_\odot$ AGB model from which the 0.89 $M_\odot$ PNN

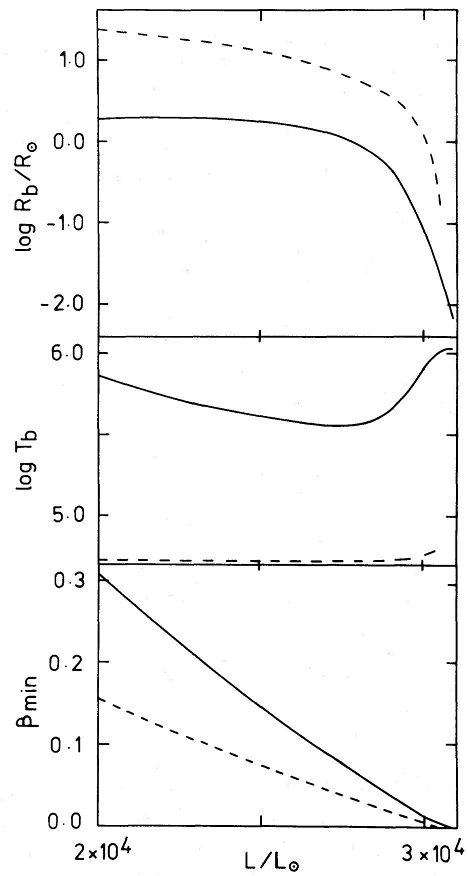

FIG. 3.—Minimum value of β ($\beta_{\rm min}$), temperature (T_b) at the base of the convective envelope, and radius (R_b) at the base of the convective envelope plotted against luminosity for stars with a core mass of 0.89 $M_\odot$ and total masses of 2 $M_\odot$ (*solid line*) and 0.9 $M_\odot$ (*dashed line*).

was extracted was still managing to hold together (although it was experiencing increasing convergence difficulties in the envelope during surface luminosity maxima; these difficulties prevented our evolving the AGB star to larger M_c values in order to study PNNi of greater mass than 0.89 $M_\odot$). However, when the envelope mass was reduced to a small value, we could no longer find a hydrostatic solution and convergence failed. We note that the dependence of Eddington limit on envelope mass is small, and we expect that our 2 $M_\odot$ AGB model would itself fail to converge (eject its envelope) if evolved only slightly further up the AGB.

The instability we have encountered here has been noted previously by Rose and Smith (1972), who also studied envelopes surrounding a core of just under 0.9 $M_\odot$. We are not aware, however, of any published report of the instability for flash calculations involving large core masses.[1] The reason is that shell flash calculations with $M_c > 0.89$ $M_\odot$ seem to have been made only in relatively massive stars with $M > 3$ $M_\odot$. Two effects combine here to save the envelope: first, and most importantly, the peak surface luminosity in such stars does not exceed the quiescent hydrogen-burning luminosity as it does in

[1] Iben (private communication) has encountered a lack of convergence after the first flash in some unpublished sequences of more massive AGB stars with $M_c = 1.2$–1.4 $M_\odot$.

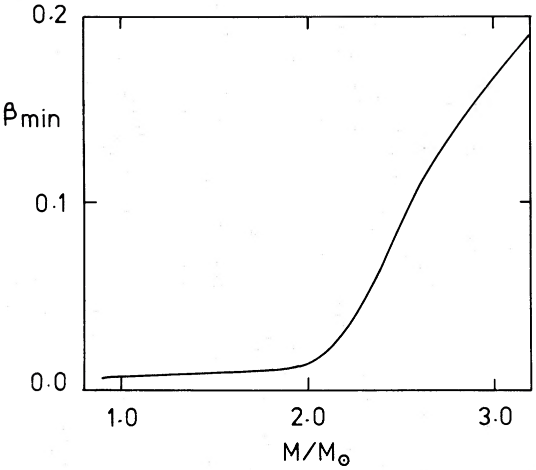

FIG. 4.—The minimum value of β at the base of the convective envelope plotted against total stellar mass for stars with core mass 0.89 $M_\odot$ and surface luminosity $3 \times 10^4 L_\odot$.

low-mass stars[2] (e.g., Weigert 1966; Iben 1975), and second, β_{min} increases with envelope mass (because of higher opacity at the envelope base) so that higher luminosities are required to produce instability. This result is shown in Figure 4, where β_{min} is plotted against total mass for a star with $M_c = 0.89\ M_\odot$ and $L = 3 \times 10^4\ L_\odot$ (appropriate for the surface luminosity maximum following a shell flash in a low-mass star).

One factor not considered above is the energy requirement for envelope ejection. It is well known (e.g., Paczyński 1969) that the total energy (thermal and ionization energy [positive] and gravitational energy [negative]) of the envelopes under consideration here is positive. To demonstrate that ample energy is available for envelope ejection, we will consider only the gravitational energy requirements. Our envelope models show that, for flash peak luminosities corresponding to a core mass of $\sim 0.89\ M_\odot$, most of the envelope mass is concentrated around 600 $R_\odot$ before ejection. To remove 1 $M_\odot$ of matter from there to infinity would require $\sim 6.4 \times 10^{45}$ ergs of gravitational energy. Using the prescriptions for time scale of the flash surface luminosity peak given in Wood and Zarro (1981), we find that for $M_c = 0.89\ M_\odot$, $\sim 1.7 \times 10^{47}$ ergs of energy are radiated from core to envelope, while the peak luminosity is within 10% of its maximum value. Hence, $\sim 4\%$ of this energy would be sufficient to supply the gravitational potential energy needed to remove 1 $M_\odot$ of the envelope totally. Such a requirement does not seem unreasonable, especially when the internal thermal energy of the envelope is considered.

A number of authors have postulated the existence of the radiation pressure instability encountered here and have carried out limited studies of the ejection process (Faulkner 1970; Sparkes and Kutter 1972). Hydrodynamical models of the envelopes of AGB stars show them to be violently unstable to pulsational instability before the radiation pressure instability sets in (Keeley 1970*b*; Smith and Rose 1972; Wood 1974; Tuchman, Sack, and Barkat 1978). These calculations suggest that high mass-loss rates will set in before the hydrostatic luminosity limits are reached; the so-called superwind may well be driven by these pulsations. Our present hydrostatic considerations may be used to define upper limits to the luminosity and core mass attainable for AGB stars and PNNi, but further detailed studies of the ejection process are clearly required.

We will now explore the hydrostatic mass and luminosity limits in greater detail. The mean value of κ in equation (2) can be roughly approximated by the electron scattering value $0.2(1 + X)\ \mathrm{cm^2\ g^{-1}}$. For low-mass stars at the peak of a helium shell flash, the luminosity and core mass are related by (Wood and Zarro 1981)

$$\frac{L}{L_\odot} = 97{,}000\left(\frac{M_c}{M_\odot} - 0.52\right).$$

Substituting these values in equation (2) gives

$$\frac{P_{\rm rad}}{P} = 1.5(1 + X)\left(1 - \frac{0.52}{M_c/M_\odot}\right). \tag{3}$$

When $P_{\rm rad}/P = 1$, the envelope is just on the verge of being lifted off by radiation pressure; it can be seen from equation (2) that this occurs just as the luminosity reaches $L_{\rm Ed}$. If $X = 0.68$, we find from equation (3) that complete hydrogen envelope ejection in low-mass AGB stars will occur when M_c reaches 0.86 $M_\odot$ and the peak flash luminosity reaches 33,000 $L_\odot$. In actual calculations we found that the envelope was stable in a 0.76 $M_\odot$ PNN at the helium shell flash but that the envelopes in PNNi of 0.86 and 0.89 $M_\odot$ suffered convergence failure in the hydrostatic code and would therefore be ejected; these results agree well with the above analytic value of the limiting mass for stable hydrogen envelopes.

For AGB stars or PNNi, the maximum luminosity in the interflash phase is given by (e.g., Wood and Zarro 1981)

$$\frac{L}{L_\odot} = 59{,}250\left(\frac{M_c}{M_\odot} - 0.495\right).$$

In this case, we find that radiation pressure will eject all the hydrogen-rich layers on a PNN only when $M_c > 1.48\ M_\odot$. This mass is larger than the maximum possible core mass for an AGB star, which is equal to the Chandrasekhar limiting mass of $\sim 1.4\ M_\odot$ for carbon-oxygen white dwarfs. Thus it is only by virtue of the higher luminosity resulting from the helium shell flashes that an AGB star of core mass greater than 0.86 $M_\odot$ can undergo Eddington limit radiation levitation of its envelope.

The radiation pressure planetary shell ejection mechanism we have been describing produces quite a clean break at the interface between the hydrogen-rich and helium-rich (CNO cycle processed) material in the progenitor AGB star. In order for the (almost) pure *helium* layers to be pushed off by radiation pressure, a core mass of 1.56 $M_\odot$ would be required according to the prescriptions above (the larger core mass results from the reduction in X). Once again, this mass is greater than the Chandrasekhar limiting mass; hence radiation pressure should not remove the pure helium layers of PNNi.

Any AGB star which attains a core mass of $\sim 0.86\ M_\odot$ will suffer one of two possible fates. (i) If the star is more massive than $\sim 3\ M_\odot$, then its shell flashes will not result in a peak surface luminosity in excess of the interflash value, and such a star, in the absence of mass loss, will proceed to become a supernova when its core mass becomes greater than the Chan-

[2] Iben (private communication) has found that, whereas this is true for several cycles after the onset of helium shell flashing in the more massive AGB stars, they too eventually begin to acquire flash-induced surface luminosity maxima greater than the interflash luminosity maxima if the evolution is continued to high enough flash cycle number. Whether such surface luminosity maxima at flash would be as luminous as in lower mass AGB stars (see below) remains to be determined.

drasekhar limit of $\sim 1.4\ M_{\odot}$. (ii) If the AGB star is less than $\sim 3\ M_{\odot}$, then the Eddington limit *will* be reached during helium flashes, and radiation pressure ejection of the envelope will ensue. It is possible, of course, that an AGB star which is *initially* of mass greater than $\sim 3\ M_{\odot}$ may be subject to enough stellar wind mass loss to change its fate from the former to the latter category. We note that the current superwind mass-loss rate estimates of $\sim 10^{-4}$ to $\sim 10^{-5}\ M_{\odot}\ \mathrm{yr}^{-1}$ mean that the duration of ejection of 1–2 $M_{\odot}$ of envelope material is sufficiently long ($> 10^4$ yr) that a helium shell flash will be encountered during this phase (the time interval between shell flashes is < 6000 yr for $M_c > 0.86\ M_{\odot}$). Thus ejection in the more massive AGB stars may be a two stage process: first, mass loss by a steady wind giving rise to reduced envelope mass, and second, a complete ejection of the hydrogen envelope during a surface luminosity peak associated with a helium shell flash.

We note that PNNi produced by the radiation pressure process (whether preceeded by stellar wind mass loss or not) will evolve into the PN domain initially burning helium; i.e., final ejection will occur at a helium shell flash. We suggest that at least some of the helium-rich PNNi and their progeny, the DB white dwarfs, are produced in this way. Indeed, all AGB stars which produce core masses greater than 0.86 $M_{\odot}$ should produce a helium-rich PNNi (or a supernova explosion).

The maximum masses for PNNi with hydrogen-rich surfaces derived above are subject to some uncertainty. For example, the approximation of $\langle \kappa \rangle$ by the electron scattering opacity is a slight underestimate of the true value of $\langle \kappa \rangle$, and a different abundance of hydrogen in the envelope will lead to a different electron scattering opacity and to different values of the peak and quiescent luminosities in a PNN of given mass (Wood 1981).

Finally, in order to circumvent the convergence problem in our 0.89 $M_{\odot}$ model we artificially stripped off all the remaining hydrogen-rich material from the starting model and tried to evolve the resulting star to the white dwarf domain. We found no difficulty in doing so. This is a clear indication that it is solely the presence of the hydrogen-rich envelope that causes the lack of convergence we encountered. The track for this test calculation has been included in Figure 1*d*, and it will be seen that the star continued to burn helium during the crossing as did the lower mass stars shown in the same panel.

c) Sequences Exhibiting a Final Helium Shell Flash

As noted above, a final mixing helium shell flash was encountered on the fading part of the H-S track in one of the sequence calculations in our main set—the case A mass-loss evolution of the 0.6 $M_{\odot}$ PNN which left the AGB at $\phi = 0.75$. In addition, PNN flashes on the horizontal part of the PNN track were found in a few of our 0.6 $M_{\odot}$ test sequences with intermediate mass loss. This occurred because lower initial rates of mass loss were employed in some of these tests, which resulted in the PNN models remaining near the AGB for much longer than was the case in our standard sequences; thus they had time to evolve into the next flash before all nuclear burning was extinguished. Figure 5 provides the H-R diagrams for all of our sequences which experienced a helium flash after leaving the AGB; the tracks *a–d* are in order of increasing departure from the AGB at the time when the flash occurred.

Table 2 provides relevant data for these sequences. The fraction of the star's mass remaining as hydrogen provides a measure of the extent to which mass loss has reduced the envelope at the epoch of the flash. This is correlated with the star's progress along the H-S track at that epoch. The ϕ value at which this last flash occurred has been calculated by relating the time of flash to the times of the surrounding two flashes that occurred in the original AGB sequence from which the starting models were derived. It appears that these final flashes occurred somewhat earlier than would have been the case had the star not been subject to the PN mass loss.

TABLE 2

DATA FOR HELIUM FLASHES OCCURRING IN 0.6 $M_{\odot}$ PNN MODELS

SEQUENCE	*a*	*b*	*c*	*d*
M_H/M	0.00393	0.00390	0.00089	0.00030
log T_{eff} (flash)	3.639	3.640	4.794	(5.155)
ϕ (flash)	0.993	0.937	0.914	0.935

NOTES.—M_H is the mass of hydrogen left on the star, log T_{eff} (flash) is the effective temperature at peak helium burning, and ϕ (flash) is the phase at which the flash occurred relative to the original AGB flash cycle.

The flash in sequence *a* occurred when the PNN had barely left the AGB. It caused two large excursions to hotter effective temperatures, each of which was followed by a return (nearly) to the AGB. Such excursions are well known to be associated with the occurrence of a flash on the horizontal part of the H-S track (Schönberner 1983; Iben 1984). The flash of sequence *b* occurred scarcely later than that of track *a*, but the small amount of additional mass loss had a marked effect on the character of the second blueward excursion; no recovery to the AGB occurred in this case and the hydrogen-burning simply took over again at about the coolest part of the true PNN domain (log $T_{\mathrm{eff}} = 4.5$). In sequence *c* the star had evolved to high enough temperature for it to ionize the nebula before the occurrence of the flash. Nevertheless, there was still a single excursion back nearly to the AGB. Sequence *c* is distinguished from the previous two cases, however, in that the second return toward the AGB (that which was only just apparent in sequence *b*) was now entirely absent. In fact, the hydrogen-burning shell never recovered in sequence *c*, and the star entered its gravitational contraction phase directly from the post-flash helium burning.

In all cases where the final flash occurred on the horizontal part of the H-S sequence the initial blueward temperature excursion was accomplished extremely rapidly (in only a few hundred years) before the energy released by helium burning had diffused to the surface. It is very unlikely that PNNi will be observed in this rapid evolutionary phase, which is terminated when the energy released in the interior diffuses to the surface and drives the star to high luminosity back on the AGB. Following this the star evolves at a much slower rate, comparable with that for the tracks obtained with no final helium flash.

Mixing flashes on the fading branch of the H-S sequence, such as that of our sequence *d*, were first predicted by Fujimoto (1977) and found in an actual sequence by Schönberner (1979). We have not followed the evolution of our sequence *d* model beyond the flash point. Iben *et al.* (1983) have developed a method of bypassing the complex flash mixing in order to investigate the subsequent evolution. Their results, for a 0.6 $M_{\odot}$ PNN, indicate that the star returns to the horizontal part of the H-S sequence again in ~ 100 yr and thereafter virtually retraces its previous track, except that it now burns helium instead of hydrogen. The time scale for this second H-S evolution is about twice that of the first. Just how far back toward

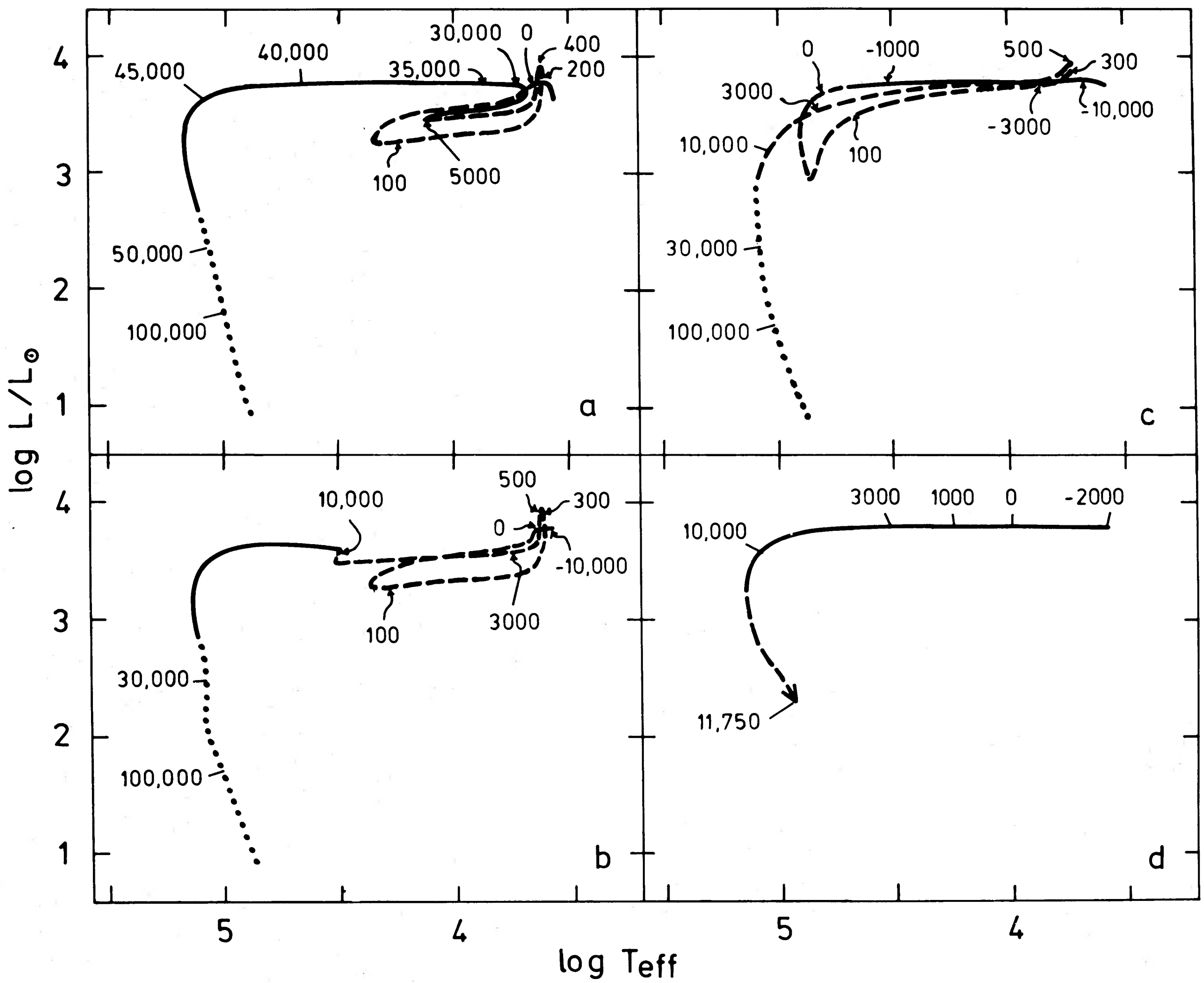

FIG. 5.—Evolutionary tracks for 0.6 $M_{\odot}$ PNN models which experienced a final helium shell flash after leaving the AGB. Hydrogen-burning phases are shown as thick lines, helium-burning phases as broken lines, and gravitational contraction phases as dotted lines. Panels are arranged in order of increasing departure from the AGB at flash. The times in panels *a–c* have their zero set at the epoch of greatest helium-burning luminosity in the flash; those of panel *d* have their zero at the log $T_{\rm eff} = 4.0$ point.

the AGB the star rejoins the horizontal part of the H-S track after a mixing flash depends very sensitively on the mass left in the hydrogen envelope and on how far its fading had progressed at the time the flash occurred (Iben 1984).

All the evolutionary tracks described in this subsection are in qualitative agreement with those obtained under similar circumstances by Iben (1984), thus providing general support for the results of his detailed study of PNN flash phenomena at 0.6 $M_{\odot}$. Time scale differences between our models and those of Iben are discussed in the next section.

d) Time Scale Considerations

As mentioned in § III*a*, the evolutionary tracks for $\phi = 0.25$, 0.50, and 0.75 at a given mass are generally similar. However, time scale differences are apparent in two evolutionary stages: (1) the transition from the AGB to the planetary nebula region and (2) early in the stage of luminosity decline. We will now discuss these two stages in turn.

The time taken for a star to transit from the AGB to the planetary nebula region is simply $t_{\rm tr} \approx (M_{\rm eR} - M_{\rm eN})/\dot{M}$, where $M_{\rm eR}$ is the envelope mass left at the end of the main mass-loss phase, $M_{\rm eN}$ is the envelope mass when $T_{\rm eff}$ increases to $\sim 3 \times 10^4$ K, and $\dot{M}$ is the rate of envelope mass decrease due to nuclear burning and mass loss (Schönberner 1979; Iben and Renzini 1983). $M_{\rm eN}$ is quite well determined by stellar evolution calculations, and the main uncertainties in $t_{\rm tr}$ are due to uncertainties in $M_{\rm eR}$ and $\dot{M}$. We do not wish to give a general discussion of values of $t_{\rm tr}$ (this has been done by Iben and Renzini 1983); but we wish to raise a point relating to $M_{\rm eR}$ which has not been discussed before.

It has generally been assumed that high mass-loss rates will cease when a star moves significantly away from the AGB, say to log $T_{\rm eff} \approx 3.7$ or 3.8; $M_{\rm eR}$ has usually been defined at this point. However, in a star of a given core mass, $M_{\rm eR}$ depends on luminosity. Increasing the luminosity causes the star to move closer to the AGB (that is why PNNi suffering post–AGB shell flashes return to the AGB). Now suppose we have a star in which the superwind ceases during the time of suppressed surface luminosity following a helium shell flash. During subsequent evolution, the surface luminosity rises toward the interflash maximum, producing a tendency for the star to return to the AGB, thereby prolonging the AGB to PNN transition. This is clearly seen in Figure 6, in which is shown the evolutionary track for a 0.6 $M_{\odot}$ PNN which left the AGB at phase 0.25 of the shell flash cycle, and in which the (type A) mass loss was discontinued at log $T_{\rm eff} = 3.8$. Since the rate of

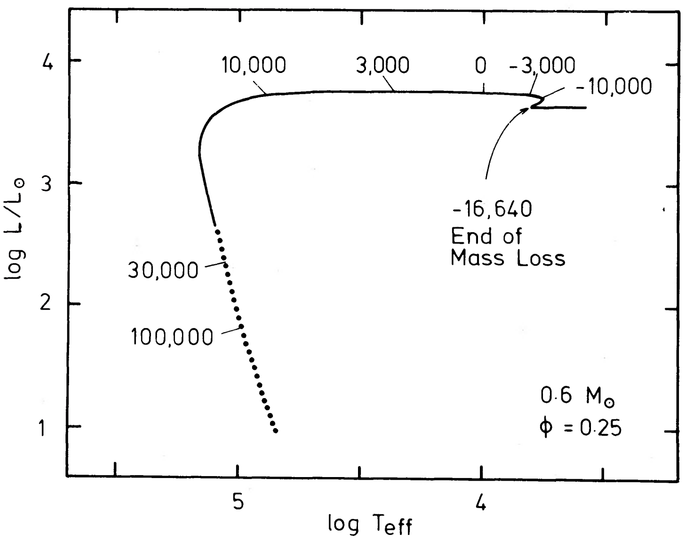

FIG. 6

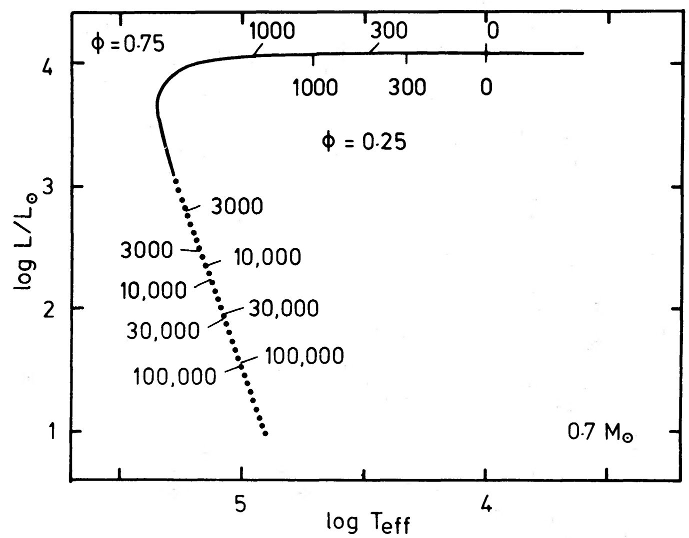

FIG. 7

FIG. 6.—Evolution of a PNN of mass 0.6 $M_\odot$ which left the AGB at phase 0.25 of a shell flash cycle

FIG. 7.—Evolution of two PNNi of mass 0.7 $M_\odot$ which leave the AGB at phases of 0.25 and 0.75 of the shell flash cycle. The two tracks are indistinguishable except for time scale of evolution. Times marked below and to the right of the evolutionary tracks correspond to the model which left the AGB at phase 0.25.

luminosity rise is greatest early in the shell flash cycle, the lengthening of t_{tr} is greatest there. The transition times given in Table 1 for models with type A mass loss clearly demonstrate this effect in the 0.6 $M_\odot$ models. The lengthening of the transition time for stars leaving the AGB early in the interflash phase is much less pronounced at higher masses. Note that for small core masses ($\sim 0.6\ M_\odot$) the delay in transition from AGB to PN, caused by the increase in quiescent, hydrogen-burning luminosity, can be a large fraction of the expansion lifetime of a PN shell. For example, the 0.6 $M_\odot$ model which leaves the AGB at $\phi = 0.25$ has $t_{tr} \approx 2 \times 10^4$ yr. Thus if superwind mass loss terminates at a random phase of the shell flash cycle, the above effect will mask what might otherwise be a tight correlation between the typical radius of a PN and position of the PNN along the evolutionary track.

The second time scale effect we wish to consider is that of the ejection phase ϕ on evolution within the PNN region of the HR diagram. Figure 7 shows the evolution of two 0.7 $M_\odot$ PNNi which left the AGB at phases 0.25 and 0.75, respectively. The evolutionary tracks of these two objects are essentially indistinguishable in the HR diagram but the time scales are somewhat different, particularly at intermediate ages on the fading part of the track. A general feature of the evolution is that the earlier in the shell flash cycle a star leaves the AGB, the slower is its rate of evolution as a PNN. The age at a given luminosity in the early fading phase varies by factors of ~ 2 for stars leaving the AGB at phases $\phi = 0.25$ and 0.75. Time scale information for different masses and phases is given in Table 1.

Finally, it is worthwhile comparing time scales for our 0.6 $M_\odot$ tracks with those for similar tracks by Schönberner (1981) and Iben (1984). For those PNN which leave the AGB during the interflash period, our time for evolution at high luminosity on the horizontal portion of the evolutionary track from $\log T_{eff} = 4.0$ ($\sim 12{,}000$ yr) is intermediate between that of Schönberner (~ 7000 yr) and Iben ($\sim 18{,}000$ yr). On the fading part of the track, our models are slowest, evolving down to $\log L/L_\odot \approx 2.3$ at $t = 3 \times 10^4$ yr after $\log T_{eff}$ reaches 4.0, while Schönberner's models evolve to $\log L/L_\odot \approx 1.9$ and Iben's to $\log L/L_\odot \approx 1.8$ in the same time. These differences presumably result from the various stars leaving the AGB at different phases of the shell flash cycle, from different input physics (e.g., abundance), and from different computer codes.

A very significant time scale difference is apparent between our calculations for a 0.6 $M_\odot$ model leaving the AGB at a shell flash and the similar calculation of Iben (1984). For example, our model reaches its peak hydrogen burning luminosity $\sim 1.8 \times 10^4$ yr after passing beyond $\log T_{eff} = 4.0$, while Iben's model (see his Fig. 1) takes $\sim 6 \times 10^4$ yr to reach the same stage. This difference in time sale is due in large part to differences between the interflash time scales of our AGB models and those of Iben (1982) from which he derived his PN model. As hydrogen reignition after a shell flash occurs at a reasonably well-defined phase in the shell flash cycle, a longer flash cycle will mean a longer time before reignition of hydrogen. Iben's interflash time Δt is given by $\log \Delta t \approx 5.4$ while ours is $\log \Delta t \approx 4.8$, in good agreement with the compilation of Becker and Iben (1980). Shell flash calculations that we have produced indicate that a factor of ~ 2 of the difference in Δt between our models and those of Iben (1982) can be accounted for by composition differences.

IV. COMPARISON WITH OBSERVATIONS

We now discuss the relationship of our calculated sequences to the observed evolutionary properties of PNNi, to see if these properties place any constraints upon the nature of the shell ejection process. Our first comparison involves location of the nuclei in the H-R diagram.

Figure 1 shows the luminosity and T_{eff} values derived observationally for PNNi in two recent surveys (Pottasch 1983; Kaler 1983). The Kaler survey was of the nuclei of PNe with large shells (radius > 0.175 pc). Some of his points represent only limiting positions for the nuclei (because of unresolved questions of optical thickness). Pottasch, on the other hand, selected his objects with a view to compiling his H-R diagram with as little recourse as possible to such "astrophysical" assumptions as that of a standard shell mass in the Shklovsky method of distance determination. In practice he used several different methods of determining both the distance and the temperature of the nucleus, so that the selection criteria implicit in his choice of objects are very complex indeed.

Taking these results at face value, particularly the luminosities obtained by Pottasch, we might conclude that the PNNi have masses below 0.6 $M_\odot$. These observed luminosities, however, appear discordant with several other observational results. In particular, they appear to indicate a PNN evolution away from the AGB at luminosities less than those characteristic of globular cluster giant branch tips (e.g., those of the 47 Tuc Miras) and much less than those of typical Galactic disk Mira variables with periods of ~ 375 days. (The Mira luminosities are based on typical luminosities for LPVs in the Magellanic Clouds [e.g., Wood, Bessell, and Paltoglou 1984]; the typical Mira period is based on the period distribution in Wood and Cahn 1977.) Since the bulk of the PNe near the Sun comes from stars more massive than those on globular cluster giant branches and probably from stars similar to typical Mira variables, they must have had AGB luminosities as high as those shown for these objects in Figure 1. The Mira AGB luminosities are a factor of ~ 3 higher than the luminosity of the horizontal part of the observed H-S sequence, as indicated by the points of Figure 1. In view of the well-known difficulties of calibrating the several distance scales for PNe and also of the assumptions implicit in these scales (particularly the assumption of the Shklovsky scale that the PN is optically thin for hydrogen-ionizing radiation), we suggest that, in spite of Pottasch's endeavor to obtain data free of astrophysical assumptions, the observational luminosities of PNNi depicted in Figure 1 may be systematically too low by a factor of ~ 3. Because of the large uncertainty in the luminosities of PNNi, it seems difficult to deduce their properties from a figure such as Figure 1.

An alternative approach is to compare the time scales of the PNN model sequences with those obtained observationally from the shell radii using some assumption concerning the shell expansion. This is done most conveniently in the (M_V, time) plane of Figure 2. Abell (1966) first explored the location of the PNNi in such a plane, but observational diagrams of this type have been produced more recently by, e.g., Schönberner (1981), Heap (1983), and Pottasch (1983). We have attempted time scale comparisons using only the *slopes* of the loci in the (M_V, time) plane, for the reasons outlined in § III*a*.

The results of our work are shown in Figure 2, where panels *a*–*d* give the time scales of our tracks as already described. Figure 2*e* reproduces the observational material derived by Schönberner (1981); see his Figure 7. Schönberner interprets these data as supporting the existence of a single tight evolutionary sequence for the PNNi, although the evidence for such a tight sequence looks far less convincing in the (M_V, *t*)-plane than in his (M_V, log *t*)-plane. In Schönberner's view the planetaries have a very narrow range of intrinsic starting properties (e.g., shell mass, PNN mass, ejection duration, etc.), and the range of observed properties is due solely to the evolutionary development of the "standard" object with time. Thus it is possible for Schönberner to derive a locus in the (M_V, *t*)-plane which separates PNe which are optically thick for Lyman radiation from those that are optically thin (see his paper for details); his locus is reproduced in Figure 2*e* as the dot-dash line. Points falling to the left of or above this line represent PNe which are optically thick; for these objects the shells will not be fully ionized, and the expansion times derived from their apparent shell radii will be too small. Schönberner found, as required by his hypothesis, that those of the PNe which he concluded to be optically thick all precede those he found to be optically thin on his evolutionary sequence. We have used his Figure 2*a* to map onto our Figure 2*e* those of his optically thick objects which fall within its boundaries; they all appear at the top left corner.

For comparison with the results of Schönberner, we have reproduced in Figure 2*f*, the observational material derived by Pottasch (1983), using his Figure 7*b*, (in which he uses his own distance scale). The dissimilarity of the distributions of these two sets of observational points casts immediate doubt on our ability to draw any definitive conclusions from comparisons between theory and observation in the (M_V, *t*)-plane, given the present state of the observational data.

The reasons for the difference between these two distributions lie partly in selection effects and partly in the assumptions employed in deriving the observational results. Schönberner selected his objects from lists of planetaries with *UBV* photometry for the nuclei. He will thus have selectivity excluded PNe with very faint nuclei and PNe with compact bright shells which make photometry of the nucleus difficult. As already mentioned, the selection criteria implicit in Pottasch's work are very complex. Another point of difference between Schönberner and Pottasch is that the former converted nebula radius into time using a standard shell expansion velocity of 20 km s^{-1}, whereas the latter used velocities as measured for the individual shells. Finally, Schönberner used Shklovsky distances, while the results of Pottasch which are reproduced here utilize Pottasch's own distances. The combined Pottasch and Schönberner samples of PNNi may well make up a more representative sample of PNNi than each sample individually.

There are a few points we wish to make about the theoretical and observational data in Figure 2.

1. In Pottasch's sample of PNNi, there are nebulae which fall in the optically thick part of Figure 2 at all values of M_V (this would be true even after correcting Pottasch's distance scale as suggested above). Such a situation is inconsistent with the interpretation favored by Schönberner in which the PNNi in the (M_V, time) diagram effectively lie on a single evolutionary sequence corresponding to a very small range in stellar mass. In this case, we would expect all the optically thick PNNi to lie at the high-luminosity, small-age end of the sequence. In view of the dependence of transition time on the phase ϕ of the shell flash cycle at which the "superwind" mass loss ceases (see § III*d*), and assuming that stars leave the AGB at more-or-less random ϕ, we would not expect a simple relation between M_v and (kinematic) age for PNNi.

2. In Pottasch's sample, there is no paucity of objects between $M_V = 4$ and 5 as found by Schönberner, who also noted that this luminosity range corresponded to a relatively rapid evolutionary phase which occurs at the end of hydrogen shell burning in PNNi. If such a gap were real, it would, according to Schönberner's arguments, tend to favor the interpretation of PNNi as stars of a small mass and mass range which left the AGB in the interflash phase and which suffered little mass loss during post–AGB evolutionary phases. The large number of optically thick stars in Pottasch's sample tends to suggest that PNNi are not mostly low-mass ($M \approx 0.6\ M_\odot$) stars.

3. The positions in Figure 2 of stars in the combined Pottasch-Schönberner sample indicate directly that PNNi cover a considerable mass range. For example, the bright ($M_V < 3$), older (age > 5000 yr) nebulae in the top part of Schönberner's diagram must have low mass ($M \approx 0.6\ M_\odot$) in

order to maintain their visual luminosities at their ages. On the other hand, the young (age < 10,000 yr), low-luminosity ($M_V > 4$) nuclei must have masses of 0.8 $M_\odot$ or greater; in particular, it would seem impossible for PNNi to acquire the lowest luminosities evident in Figure 2 ($M_V > 7$) at any time while the associated shell is still visible ($t < 30{,}000$ yr) unless they are massive. Renzini (1981), from a comparison of earlier observational data for PNNi in the H-R diagram and previously calculated evolutionary time scales, also concluded that PNNi span a range of mass.

4. Evolutionary tracks for PNNi leaving the AGB in both flash and interflash phases of evolution can explain the distribution of observational data in the (M_V, time) diagram. A track of given slope in the (M_V, time) diagram could be ascribed to a PNN of some mass which leaves the AGB at a helium shell flash or equally to a somewhat less massive (by $\sim 0.1\ M_\odot$) PNN which leaves the AGB in the interflash phase.

5. An observational constraint on the mass-loss process in PNe may be provided by the properties of the DA white dwarf variable stars of type ZZ Cet (Winget and Fontaine 1982). There is a distinct temperature interval on the white dwarf cooling sequence in which *all* the DA white dwarfs pulsate. Furthermore, according to Winget and Fontaine (1982), theoretical linear pulsation models for these stars indicate that the sharp blue edge and the narrowness of the strip may be explained only if the hydrogen content of the DA stars has been reduced to $\sim 10^{-9}$ of their mass. However, these results have recently been disputed by Cox *et al.* 1985, who find that white dwarfs can pulsate with much larger amounts of hydrogen on their surfaces. If the Winget and Fontaine results are correct, *all* DA white dwarfs have less than 10^{-9} of their mass left as hydrogen by the time they have cooled to $T_{\rm eff} = 11{,}000$ K. Since the DB stars appear to have no hydrogen left at all, this implies an upper limit to the amount of hydrogen remaining for *all* stars as they enter the white dwarf domain. We have found that a PNN evolving with no further mass loss in the PNN domain (Fig. 2*a*–*b*) becomes a white dwarf with a remaining hydrogen-rich envelope which violates the ZZ Cet limit by several orders of magnitude, a point noted previously by Faulkner and Wood (1984) and Iben and Tutukov (1984). We are therefore forced to the conclusion that all PNNi do suffer continuing mass loss during the PNN phase or that the results of Cox *et al.* (1985) are correct and that white dwarfs can indeed pulsate when the mass of hydrogen on their surfaces greatly exceeds $10^{-9}\ M_\odot$. Mass loss is certainly detected observationally in a reasonable fraction of PNNi (Perinotto 1983). Comparing panels *a* and *b* of Figure 2 with panels *c* and *d* we see that when mass loss is continued into the PN domain, the difference between the fading times of PNNi leaving the AGB at the flash and in the interflash is enhanced, while the fading times for flash models are relatively unaffected by mass loss.

We next examine the suggestion that at least some of the DB white dwarfs and helium PNNi are the more massive PNNi ($M > 0.86\ M_\odot$) which undergo helium shell flashes at or after shell ejection. Mass determinations for DB white dwarfs and helium PNNi are at present very poor. Shipman (1979), Koester, Schulz, and Weidemann (1979), Koester, Schulz, and Wegner (1981), Wickramasinghe and Reid (1983), and Oke, Weidemann, and Koester (1984) have derived masses for solar neighborhood samples of DA and DB white dwarfs and find that there is no evidence for a significant difference between the masses of the two subtypes (see also Weidemann and Koester 1983). The DA stars have a ($\pm 1\ \sigma$) mass range of $0.58 \pm 0.10\ M_\odot$, and the less well observed non–DA dwarfs yield similar results. Some particular white dwarfs of greater than average mass, associated with open clusters of age $\sim 10^8$ yr, have, in fact, been observed to have DA rather than DB spectra. Weidemann and Koester (1983) describe three such stars in NGC 2516 and (possibly) one in NGC 2422, which have evolved from progenitors of masses 7–10 $M_\odot$ and have present masses of 0.9–1.2 $M_\odot$. It is possible, however, that an initially helium-rich PNN could accrete sufficient hydrogen-rich material during its cooling age for it to appear as a DA dwarf. Using Bondi's (1952) accretion approximation, we find that, if there were a cold (100 K) neutral gas cloud with number density 10 cm^{-3} associated with the cluster, and if a 1 $M_\odot$ white dwarf had a velocity with respect to the gas typical of the velocity dispersion in an open cluster, say 2 km s^{-1}, then such a star might be expected to accrete $\sim 10^{-4}\ M_\odot$ over the 5×10^7 yr cooling time (to 30,000 K) of the DA dwarfs in NGC 2516. This is many orders of magnitude greater than the mass of the white dwarf atmosphere (Strittmatter and Wickramasinghe 1971). In fact, the problem with DB white dwarfs lies in explaining how *any* of them can survive with hydrogen-free atmospheres in the normal interstellar medium for times longer than a few thousand years (see Liebert 1980 and references therein). Thus the existence of more massive DA white dwarfs is not necessarily harmful to our hypothesis, although a result indicating low masses for *all* DB dwarfs would be. However, the sample of presently observed DB stars is such a limited one, and their mass estimates have sufficient uncertainties, that no definitive statement on this matter can yet be made.

The mass estimates for helium PNNi are equally uncertain. Heap (1982) has analyzed data on Wolf-Rayet (WR) PNNi (which have helium surfaces) and estimates a mean mass of $\sim 0.65\ M_\odot$, based on a mean luminosity of $\sim 9000\ L_\odot$ and a standard (luminosity, mass) relation for stars on the horizontal part of the PNN evolutionary track. These mass and luminosity estimates are greater than those of typical non–WR PNNi, and Heap suggests that it may be the high L/M ratio in the WR PNNi that drives the mass loss observed in them. Heap also notes that the kinematics of PNe containing WR nuclei indicate that these objects come from stars that are more massive than the stars that produce the non–WR PNNi. All the above results are clearly very uncertain, and further observational and theoretical results are needed to tie down the masses of PNNi and white dwarfs.

Finally, we note the possibility that the radiation pressure ejection mechanism discussed in this paper might help explain the apparent deficiency of high-luminosity ($M_{\rm bol} < -6$) AGB stars in the Magellanic Clouds; the Clouds provide an excellent testing ground between theory and observation for these late-type stars (see Iben and Renzini 1983 for a summary of the evidence for this deficiency, particularly as it relates to carbon stars). In more recent work, Reid and Mould (1984) have presented a photometric survey of a large sample of stars in a 15 deg^2 region of the LMC; they find a deficiency in the range $-6.5 < M_{\rm bol} < -5$, and an absence of the expected discontinuity in the luminosity function at the AGB limit at $M_{\rm bol} \approx -7$ (where M_c approaches the Chandrasekhar limit and a supernova results).

It is possible that this apparent deficiency in upper AGB stars in the Magellanic Clouds may be due in part to there having been specific epochs of star formation in the Clouds (e.g., Frogel and Blanco 1983; Wood, Bessell, and Paltoglou

1985); there is certainly some evidence that the luminosity function varies from region to region in the Large Cloud indicating different star formation histories (Reid and Mould 1984). It is also possible, however, that the observed deficiency is due to some additional mechanism for mass loss on the upper AGB, and the radiation pressure shell ejection discussed here could well provide just such a mechanism. We note, however, that Wood, Bessell, and Fox (1983) have found some stars having luminosities right up to the theoretical AGB limit at $M_{\rm bol} \approx -7$, indicating that it is possible for at least some AGB stars to attain core masses well in excess of 0.86 $M_{\odot}$.

V. SUMMARY AND CONCLUSIONS

We have calculated a substantial array of evolutionary sequences for PNNi of different masses, incorporating mass loss (of several forms) directly into the calculations and adopting realistic starting conditions to describe PN ejection at several different phases of the AGB helium shell flash cycle.

A critical core mass ($\sim$0.86 $M_{\odot}$) has been found for AGB stars of mass less than 3 $M_{\odot}$ (and PNNi), above which all hydrogen-rich material in the stellar envelope will be ejected by radiation pressure at a helium shell flash. If the mass of an AGB star is greater than 3 $M_{\odot}$ its fate will depend upon the effectiveness of superwind mass loss. If this reduces the stellar mass to below 3 $M_{\odot}$ before the core mass reaches the Chandrasekhar limiting mass of $\sim$1.4 $M_{\odot}$, then once again the radiation pressure mechanism is effective in causing ejection of all hydrogen-rich envelope material; if not, then a supernova will result. (In the former case, the time scale of the superwind mass loss [on current estimates] is longer than the interflash interval for AGB stars with core masses $>$0.86 $M_{\odot}$; thus a shell flash will always be encountered to activate the radiation pressure mechanism.) We suggest that this radiation levitation is the mechanism by which at least some of the DB white dwarfs and PNNi with helium surface layers are formed. It might also explain a deficiency in the number of high-luminosity AGB stars observed in some recent surveys in Magellanic Cloud fields.

For stars that leave the AGB during the interflash phase, the transition time from the AGB to the planetary nebula region varies strongly with the phase of the shell flash cycle at which the star leaves the AGB. Stars that leave early in the shell flash cycle (during the main part of the recovery from the interflash luminosity minimum) may spend a considerable fraction of their luminous post–AGB lifetime transiting to the PN domain. For example, with our mass-loss prescriptions, a 0.6 $M_{\odot}$ PNN which left the AGB at $\phi = 0.25$ took $\sim 2 \times 10^4$ yr to reach the temperature at which the surrounding nebula should develop characteristic planetary nebula emission, $T_{\rm eff} \approx 3 \times 10^4$ K.

The fading time scale for quiescent evolution does not decrease as rapidly with increasing mass beyond $\sim$0.8 $M_{\odot}$, as has previously been believed. This result implies that more massive nuclei will be observed more frequently than has usually been assumed.

Comparison of our evolutionary tracks with the observational Harman-Seaton sequence indicates that some recently published PNN luminosities may be too low by a factor of 3. A discussion of the currently available observational data for PNN evolutionary time scales [based on the (M_V, time) diagram] indicates that they are not yet sufficiently well known to allow definitive conclusions to be drawn by comparing them with the corresponding evolutionary time scales. Nevertheless, there does seem to be some evidence that the observed PNN properties result from the superposition of a family of evolutionary tracks for PNNi with a range of masses. It is possible to explain the observed distribution of points in terms of models that leave the AGB either at or between helium shell flashes.

We are grateful to an anonymous referee for prompting additional calculations which proved very helpful in elucidating the nature of the radiation pressure mechanism discussed in this paper. It is a pleasure to thank Icko Iben, Jr., for his reading of and comments on the revised manuscript.

REFERENCES

Abell, G. O. 1966, *Ap. J.*, **144**, 259.
Becker, S. A., and Iben, I. 1980, *Ap. J.*, **237**, 111.
Bondi, H. 1952, *M.N.R.A.S.*, **112**, 195.
Cox, A. N., Starrfield, S. G., Kidman, R. B., and Pesnell, W. D. 1985, preprint.
Faulkner, D. J. 1970, *Ap. J.*, **162**, 513.
Faulkner, D. J., and Wood, P. R. 1984, *Proc. Astr. Soc. Australia*, **5**, 543.
Frogel, J. A., and Blanco, V. M. 1983, *Ap. J.*, **274**, L57.
Fujimoto, M. Y. 1977, *Pub. Astr. Soc. Japan*, **29**, 331.
Gingold, R. A. 1974, *Ap. J.*, **193**, 177.
Härm, R., and Schwarzschild, M. 1975, *Ap. J.*, **200**, 324.
Harman, R. J., and Seaton, M. J. 1966, *M.N.R.A.S.*, **132**, 15.
Heap, S. R. 1982, in *IAU Symposium 99, Wolf-Rayet Stars: Observations, Physics, Evolution*, ed. C. W. H. de Loore and A. J. Willis (Dordrecht: Reidel), p. 423.
Heap, S. R. 1983, in *IAU Symposium 103, Planetary Nebulae*, ed. D. R. Flower (Dordrecht: Reidel), p. 375.
Iben, I., Jr. 1975, *Ap. J.*, **196**, 525.
———. 1982, *Ap. J.*, **260**, 821.
———. 1984, *Ap. J.*, **277**, 333.
Iben, I., Jr., Kaler, J. B., Truran, J. W., and Renzini, A. 1983, *Ap. J.*, **264**, 605.
Iben, I., Jr., and Renzini, A. 1983, *Ann. Rev. Astr. Ap.*, **21**, 271.
Iben, I., Jr., and Tutukov, A. V. 1984, *Ap. J.*, **282**, 615.
Jones, T. J., Hyland, A. R., Wood, P. R., and Gatley, I. 1983, *Ap. J.*, **273**, 669.
Kaler, J. B. 1983, *Ap. J.*, **271**, 188.
Keeley, D. A. 1970*a*, *Ap. J.*, **161**, 643.
———. 1970*b*, *Ap. J.*, **161**, 657.
Knapp, G. R., Philips, T. G., Leighton, R. B., Lo, K. Y., Wannier, P. G., and Wootten, H. A. 1982, *Ap. J.*, **252**, 616.
Koester, D., Schulz, H., and Wegner, G. A. 1981, *Astr. Ap.*, **102**, 331.
Koester, D., Schulz, H., and Weidemann, V. 1979, *Astr. Ap.*, **76**, 232.
Liebert, J. 1980, *Ann. Rev. Astr. Ap.*, **18**, 363.
Oke, J. B., Weidemann, V., and Koester, D. 1984, *Ap. J.*, **281**, 276.
Paczyński, B. 1969, *Acta Astr.*, **19**, 1.
———. 1971, *Acta Astr.*, **21**, 417.
Perinotto, M. 1983, in *IAU Symposium 103, Planetary Nebulae*, ed. D. R. Flower (Dordrecht: Reidel), p. 323.
Pottasch, S. R. 1983, in *IAU Symposium 103, Planetary Nebulae*, ed. D. R. Flower (Dordrecht: Reidel), p. 391.
Reid, N., and Mould, J. 1984, *Ap. J.*, **284**, 98.
Reimers, D. 1975, in *Problems in Stellar Atmospheres and Envelopes*, ed. B. Bascheck, W. H. Kegel, and G. Traving (Berlin: Springer), p. 229.
Renzini, A. 1981, in *Physical Processes in Red Giants*, ed. I. Iben. and A. Renzini (Dordrecht: Reidel), p. 431.
Renzini, A. 1983, in *IAU Symposium 103, Planetary Nebulae*, ed. D. R. Flower (Dordrecht: Reidel), p. 267.
Robinson, G. J., Reay, N. K., and Atherton, P. D. 1982, *M.N.R.A.S.*, **199**, 649.
Rose, W. K., and Smith, R. L. 1972, *Ap. J.*, **173**, 385.
Sabbadin, F., and Hamzaoglu, E. 1982, *Astr. Ap.*, **110**, 105.
Schönberner, D. 1979, *Astr. Ap.*, **79**, 108.
———. 1981, *Astr. Ap.*, **103**, 119.
———. 1983, *Ap. J.*, **272**, 708.
Schwarzschild, M., and Härm, R. 1965, *Ap. J.*, **142**, 855.
Seaton, M. J. 1966, *M.N.R.A.S.*, **132**, 113.
Shipman, H. L. 1979, *Ap. J.*, **228**, 240.
Smith, R. L., and Rose, W. K. 1972, *Ap. J.*, **176**, 395.
Sparkes, W. M., and Kutter, G. S. 1972, *Ap. J.*, **175**, 707.
Strittmatter, P. A., and Wickramasinghe, D. T. 1971, *M.N.R.A.S.*, **152**, 47.
Tuchman, Y., Sack, N., and Barkat, Z. 1978, *Ap. J.*, **219**, 183.

Weidemann, V., and Koester, D. 1983, *Astr. Ap.*, **121**, 77.
Weigert, A. 1966, *Zs. Ap.*, **64**, 395.
Werner, M. W., Beckwith, S., Gatley, I., Sellgren, K., Berriman, G., and Whiting, D. L. 1980, *Ap. J.*, **239**, 540.
Wickramasinghe, D. T., and Reid, N. 1983, *M.N.R.A.S.*, **203**, 887.
Winget, D. E., and Fontaine, G. 1982, in *Pulsations in Classical and Cataclysmic Variable Stars*, ed. J. P. Cox and C. J. Hansen (Boulder: JILA Report), p. 46.
Wood, P. R. 1974, *Ap. J.*, **190**, 609.
———. 1981, in *Physical Processes in Red Giants*, ed. I. Iben and A. Renzini (Dordrecht: Reidel), p. 135.
Wood, P. R., Bessell, M. S., and Fox, M. W. 1983, *Ap. J.*, **272**, 99.
Wood, P. R., Bessell, M. S., and Paltoglou, G. 1984, *Ap. J.*, **290**, 477.
Wood, P. R., and Cahn, J. H. 1977, *Ap. J.*, **211**, 499.
Wood, P. R., and Zarro, D. M. 1981, *Ap. J.*, **247**, 247.
Zuckerman, B. 1980, *Ann. Rev. Astr. Ap.*, **18**, 263.

D. J. Faulkner and P. R. Wood: Mount Stromlo and Siding Spring Observatories, Private Bag, Woden PO Act 2606, Australia